JOURNAL OF PROTEOMICS 120 (2015) 75–94

Available online at www.sciencedirect.com

ScienceDirect

www.elsevier.com/locate/jprot

Effects of heavy metals on *Cyanothece* sp. CCY 0110 growth, extracellular polymeric substances (EPS) production, ultrastructure and protein profiles

Rita Mota[a,b,c,1], *Sara B. Pereira*[a,b,1], *Marianna Meazzini*[d], *Rui Fernandes*[a,b], *Arlete Santos*[a,b,c], *Caroline A. Evans*[e], *Roberto De Philippis*[d,f], *Phillip C. Wright*[e], *Paula Tamagnini*[a,b,c,*]

[a]*Instituto de Investigação e Inovação em Saúde, Universidade do Porto, Porto, Portugal*
[b]*IBMC — Instituto de Biologia Molecular e Celular, Universidade do Porto, Porto, Portugal*
[c]*Faculdade de Ciências, Departamento de Biologia, Universidade do Porto, Porto, Portugal*
[d]*Department of Agrifood Production and Environmental Sciences, University of Florence, Florence, Italy*
[e]*ChELSI Institute, Department of Chemical and Biological Engineering, University of Sheffield, Sheffield, United Kingdom*
[f]*Institute of Ecosystem Study (ISE), National Research Council (CNR), Sesto Fiorentino (FI), Italy*

ARTICLE INFO

Article history:
Received 29 October 2014
Accepted 7 March 2015
Available online 14 March 2015

Keywords:
Cyanobacteria
Cyanothece
Extracellular polymeric substances (EPS)
Heavy metals
iTRAQ
Proteome

ABSTRACT

The effects of several heavy metals on the growth/survival, EPS production, ultrastructure and protein profiles of the highly efficient extracellular polymeric substances (EPS)-producer cyanobacterium *Cyanothece* sp. CCY 0110 were evaluated. Our results clearly show that each heavy metal affects the cells in a particular manner, triggering distinctive responses. Concerning chronic exposure, cells were more affected by Cu^{2+} followed by Pb^{2+}, Cd^{2+}, and Li^{+}. The presence of metal leads to remarkable ultrastructural changes, mainly at the thylakoid level. The comparison of the proteomes (iTRAQ) allowed to follow the stress responses and to distinguish specific effects related to the time of exposure and/or the concentration of an essential (Cu^{2+}) and a non-essential (Cd^{2+}) metal. The majority of the proteins identified and with fold changes were associated with photosynthesis, CO_2 fixation and carbohydrate metabolism, translation, and nitrogen and amino acid metabolism. Moreover, our results indicate that during chronic exposure to sub-lethal concentrations of Cu^{2+}, the cells tune down their metabolic rate to invest energy in the activation of detoxification mechanisms, which eventually result in a remarkable recovery. In contrast, the toxic effects of Cd^{2+} are cumulative. Unexpectedly, the amount of released polysaccharides (RPS) was not enhanced by the presence of heavy metals.

Biological significance
This work shows the holistic effects of different heavy metals on the cells of the highly efficient EPS-producer the cyanobacterium *Cyanothece* sp. CCY 0110. The growth/survival,

* *Corresponding author at:* IBMC — Instituto de Biologia Molecular e Celular, Universidade do Porto, Rua do Campo Alegre 823, 4150-180 Porto, Portugal. Tel.: +351 226074900; fax: +351 226099157.
E-mail address: pmtamagn@ibmc.up.pt (P. Tamagnini).
[1] Both authors contributed equally to this work.

http://dx.doi.org/10.1016/j.jprot.2015.03.004

EPS production, ultrastructure, protein profiles and stress response were evaluated. The knowledge generated by this study will contribute to the implementation of heavy-metal removal systems based on cyanobacteria EPS or their isolated polymers.

1. Introduction

Cyanobacteria are photoautotrophic prokaryotes capable of producing extracellular polymeric substances (EPS), which can remain associated with the cell surface as sheaths, capsules and/or slimes, or be released into the surrounding environment as released polysaccharides (RPS). Several roles are attributed to EPS, such as protection of the cells against desiccation, predators and UV radiation, contribution to the formation of biofilms, and/or the sequestration/immobilization of nutrients and metal ions [1,2].

Heavy metals are one of the worldwide most common causes of pollution, being a serious hazard to the environment and public health [3,4]. EPS-producing cyanobacteria or their isolated EPS can be an advantageous alternative to conventional physicochemical methods to remove heavy metals from polluted waters, since these microorganisms have minimal nutritional requirements, are easy to cultivate and exhibit rapid metal removal kinetics [5–7]. Moreover, the particular characteristics of cyanobacterial EPS make them very attractive for bioremediation. The overall negative charge of the polymer confers a high affinity towards metal cations, and the high number of different monosaccharides increases the number of possible conformations facilitating the interactions between metal ions and the EPS binding sites [2,8]. However, a successful implementation of biotechnological systems based on cyanobacteria/cyanobacterial-EPS will depend on the characteristics of the pollutant(s), the strain and/or the EPS utilized. Depending on the metal(s)/metals(s) concentration(s) and its toxic effects, it may be more advantageous to use whole cultures or the isolated EPS. Therefore, it is necessary to assess the interactions between the cells and the metal ions, e.g. if it exists an active uptake of the metal by the cells and/or a passive biosorption of the cations [9,10].

Some metals are essential to many physiological processes (e.g. copper and iron), while others are non-essential to the cell life (e.g. cadmium and lead). However, in excess, all metals are deleterious to the cells [11–13]. Several protection mechanisms have been described for cyanobacterial cells to avoid/minimize the toxicity of heavy metals. These strategies can occur extracellularly as, for example, the sequestration of metal ions on the outer cell surface or the release of ligands. However, these strategies usually need to be combined with other cellular mechanisms to achieve homeostasis, such as exporting P-type ATPases to detoxify heavy metal cations by efflux and/or the binding of these cations to metallothioneins, preventing free toxic metals [14,15]. Nevertheless, these mechanisms may not be enough to cope with the toxic effects, leading to an unbalanced oxidative state mainly by the formation of reactive oxygen species (ROS), which can result in cell death [16].

This work aimed at evaluating the effects of the presence/concentration of several heavy metals commonly found in polluted water bodies (copper, lead, cadmium and lithium) in the growth/survival, ultrastructure and EPS production by the unicellular cyanobacterium *Cyanothece* sp. CCY 0110 (hereafter referred as *Cyanothece*). This marine N_2-fixing cyanobacterium has its genome fully sequenced and is among the most efficient RPS producers [17]. In addition, the proteomes of *Cyanothece* grown in the absence/presence of copper or cadmium were compared using iTRAQ isobaric tagging technology. The results presented here will contribute to understand how the cyanobacterial cells cope with the presence and different concentrations of metals and, in the future, will help to implement metal removal systems based on cyanobacteria/cyanobacterial EPS.

2. Material and methods

2.1. Organism and culture conditions

The unicellular cyanobacterium *Cyanothece* sp. CCY 0110 (Culture Collection of Yerseke, The Netherlands) was grown in 100 ml Erlenmeyer flasks containing ASNIII medium [18] supplemented with 1 M MOPS buffer (pH 7.0), at 30 °C under a 12 h light (50 μE/m^2/s)/12 h dark regimen with magnetic stirring (150 rpm). These conditions were previously identified as maximizing *Cyanothece*'s growth and EPS production [17].

2.2. Growth curves

Cyanothece was grown during 28 days (in the case of chronic exposure) under the conditions mentioned above (control) or with the medium supplemented with different concentrations of metals: 40, 50, 60 and 70 mg/l (5.79, 7.20, 8.64 and 10.10 μM) of lithium (Li^+, stock solution 1000 mg/l in 2% HNO_3, PerkinElmer, MA, USA); 0.1, 0.2 and 0.3 mg/l (1.57, 3.15 and 4.72 μM) of copper (Cu^{2+}, stock solution 10,000 mg/l in 1% HNO_3, Sigma-Aldrich Co., MO, USA); 1, 5, 10 and 15 mg/l (4.83, 24.10, 48.30 and 72.30 μM) of lead (Pb^{2+}, stock solution 10,000 mg/l in 5% HNO_3, Sigma-Aldrich); or 1, 3, 5, 7 and 10 mg/l (8.89, 26.70, 44.50, 62.30 and 88.90 μM) of cadmium (Cd^{2+}, stock solution 10,000 mg/l in 5% HNO_3, Sigma-Aldrich). For acute exposure, *Cyanothece* cells were grown in control conditions during 9 days, followed by the addition of 1 mg/l of Cu^{2+} or 50 mg/l of Cd^{2+} and the samples were collected after 24 h. Growth measurements were performed by monitoring the Optical Density (OD) at 730 nm [19] using a SmartSpec 3000 (Bio-Rad Laboratories, Inc., Hercules, CA, USA), and chlorophyll *a* content was determined as described by Meeks and Castenholz [20]. The total carbohydrate content and the amount of carbohydrates released to the culture medium (RPS) were measured using the phenol–sulfuric acid assay [21], as described previously [17]. All experiments were performed with three biological replicates and all

measurements were performed in triplicate. Results are expressed as mean values ± standard deviation.

2.3. Transmission electron microscopy (TEM)–energy dispersive X-ray (EDX) spectroscopy

For TEM–EDX the *Cyanothece* cells were collected after 10, 20 and 30 days of culture, either in the absence of heavy metals (control) or in the presence of 0.1 mg/l Cu^{2+}, 1 mg/l Pb^{2+}, 5 mg/l Cd^{2+} or 60 mg/l Li^{+}, and after 24 h of culture in the presence of 1 mg/l Cu^{2+} or 50 mg/l Cd^{2+}. The cells were centrifuged and processed as described previously [22], except that samples were embedded in EMBed-812 resin and sections were examined using a JEM-1400Plus (Jeol Ltd., Inc., MA, USA). For EDX analysis, 100 nm thick sections were mounted on nickel grids and a beryllium holder (EM-21150, Jeol Ltd.) was used. An X-Max 80 mm^2 (Oxford Instruments, Bucks, England) operated at 80 kV was coupled to the microscope.

2.4. Atomic absorption spectroscopy

Cells were grown in ASNIII buffered medium or buffered medium supplemented with 0.1 mg/l of Cu^{2+} or 5 mg/l of Cd^{2+} (for 10 or 20 days, chronic exposure) or 1 mg/l of Cu^{2+} or 50 mg/l of Cd^{2+} (24 h, acute exposure). To measure the concentration of copper and cadmium in the supernatant, the cultures were centrifuged at 3850 *g* for 20 min at room temperature, the cells were discarded, and the concentration of the metals was determined using a flame atomic absorption spectrophotometer (PU 9200X, Philips Scientific, New Jersey, USA) operating at wavelengths of 232.00 nm for Cu^{2+} and 228.80 nm for Cd^{2+} quantification.

2.5. iTRAQ experimental design

The experiments comprised two biological replicates for each 8-plex iTRAQ independent experiment. Two iTRAQ studies were performed (see Fig. 1), namely the comparison of the proteomes of *Cyanothece* grown in the absence or presence of copper (iTRAQ study 1) or cadmium (iTRAQ study 2). The biological replicates used as control were common to the two studies (Fig. 1). Both studies comprised four phenotypes of cells grown with a 12 h light (50 $\mu E/m^2/s$)/12 h dark regimen, 30 °C and orbital shaking at 150 rpm:

(C_1, C_2) in ASNIII buffered medium for 10 days (control),
(Cu_1, Cu_2 & Cd_1, Cd_2) in medium supplemented with either 0.1 mg/l of Cu^{2+} or 5 mg/l of Cd^{2+} for 10 days (chronic exposure),
(Cu_3, Cu_4 & Cd_3, Cd_4) in medium supplemented with either 0.1 mg/l of Cu^{2+} or 5 mg/l of Cd^{2+} for 20 days (chronic exposure), and
(Cu_5, Cu_6 & Cd_5, Cd_6) in medium supplemented with either 1 mg/l Cu^{2+} or 50 mg/l Cd^{2+} for 24 h (acute exposure).

2.6. Protein extraction and quantification

The cells were harvested by centrifugation (3850 *g* for 15 min at room temperature), washed with buffer (50 mM Tris, pH 7.4, 100 mM EDTA, pH 8.0, and 25% (w/v) sucrose) and re-suspended in phosphate buffer (50 mM K_2HPO_4, 50 mM KH_2PO_4, pH 6.8). The proteins were extracted using the FastPrep^R-24 cell disruptor, output 6.5 m/s, 5 cycles of 30 s (MP Biomedicals, LCC, CA, USA) and glass beads (425–600 μm, Sigma-Aldrich) for mechanical cell disruption, followed by centrifugation at 16,000 *g* for 15 min at 4 °C. The supernatant containing the soluble proteins was recovered and stored at −80 °C. The protein concentration was measured using the BCA™ Protein Assay Kit (Pierce Biotechnology, Inc., IL, USA) and iMark Microplate Absorbance Reader (Bio-Rad Laboratories), according to the manufacturer's instructions.

2.7. Protein sample processing and peptide labeling with Isobaric tags for relative and absolute quantification (iTRAQ) peptide labeling reagents

Proteins were precipitated by adding 6 volumes of ice-cold acetone to 150 μg of the protein extract, resuspended in 20 μl of TEAB (triethylammonium bicarbonate, 1 M, pH 8.5) and denaturated by adding 1 μl of 2% SDS. Cysteines were reduced with 2 μl of tris(2-carboxyethyl)phosphine (TCEP, 50 mM) and alkylated with 1 μl MMTS (s-methyl methanethiosulfonate, 200 mM). Subsequently, the proteins were digested with trypsin as previously described [23]. The quality and amount of proteins and the efficiency of the trypsin digestion were controlled by analyzing 20 μg of protein extract in a 10% acrylamide gels. The iTRAQ labeling of the digests, and the combining of the labeled digests into one sample mixture was performed using the manufacturer's protocols (iTRAQ® Reagents — 8plex, AB SCIEX™, Framingham, MA, USA). iTRAQ labeling efficiency was 95.1% for iTRAQ study 1 (Cu^{2+}) and 95.9% for iTRAQ study 2 (Cd^{2+}). Combined samples were concentrated by vacuum (Eppendorf, Hamburg, Germany).

2.8. High-resolution hydrophilic interaction chromatography (HILIC) fractionation

Samples were resuspended in HILIC buffer A (10 mM NH_4HCO_2, 80% ACN, pH 3.0) and fractionated by HILIC using a PolyHydroxyethyl™ A column (PolyLC, Columbia, MD, USA) with 5 μm particle size, 20 cm length × 2.1 mm diameter and 200 Å pore size on a Ultimate 3000 HPLC (Thermo Scientific, formerly Dionex, Amsterdam, The Netherlands) controlled by Chromeleon Software, version 6.5 (Thermo Scientific). A set of binary gradient buffers was used for liquid chromatography: buffer A (see above) and buffer B (10 mM NH_4HCO_2, 5% ACN, pH 4.0). The binary gradient began with 0% B for 10 min, followed by a linear ramp from 0 to 60% B for 30 min, an extended ramp from 60 to 100% B for 5 min, a further isocratic wash 100% B for 10 min, and column re-equilibration at 0% B for 1 min, in a total of 66 min. Injection volume was set at 20 μl with a constant chromatographic flow rate of 0.5 ml/min. Fractions were collected using a Foxy Jr. Fraction Collector (Dionex, Sunnyvale, CA, USA) in 30 s intervals across 60 min, while the chromatogram was monitored at a wavelength of 280 nm. The fractions were cleaned using C18 UltraMicroSpin Columns (The Nest Group Inc., Southborough, MA, USA) according to the manufacturer's guidelines, prior to vacuum centrifugation (Eppendorf).

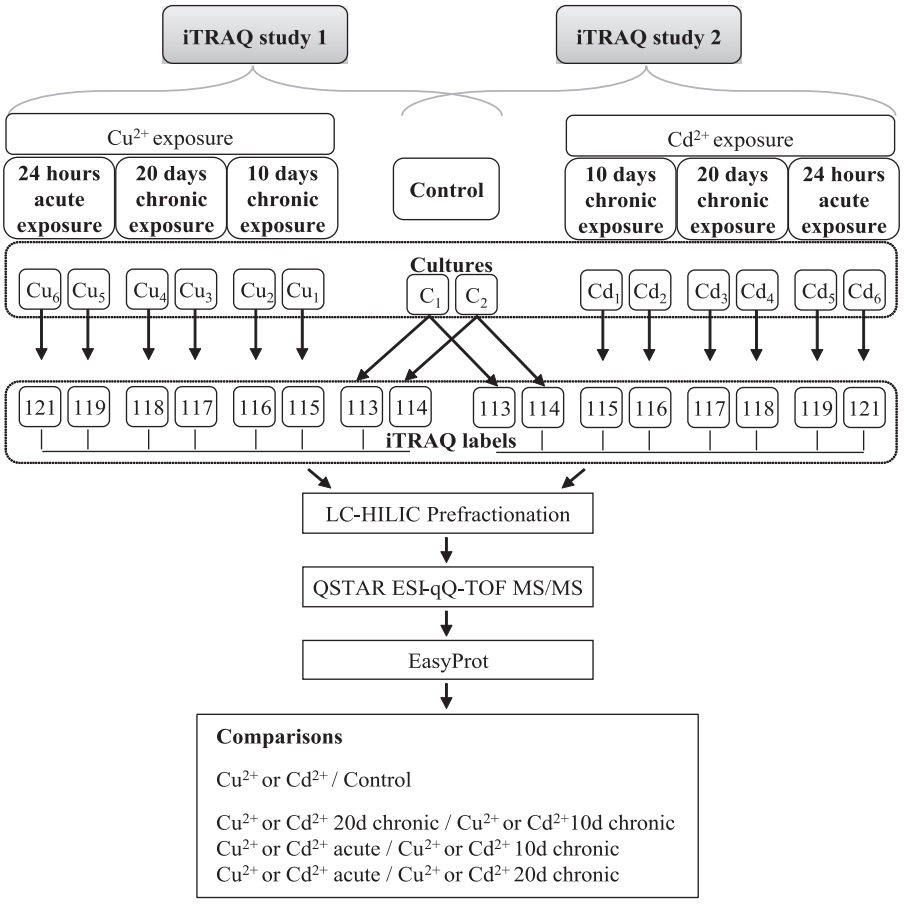

Fig. 1 – Graphical representation of the iTRAQ workflow and analyses preformed.

2.9. *Reverse phase liquid chromatography (RPLC)–MS analysis*

RPLC analysis was performed using an Acclaim^R PepMap100 C18 column (Thermo Scientific) with 3 μm particle size of 15 cm length × 75 μm diameter and 100 Å pore size on a Ultimate 3000 HPLC (Dionex), and the MS analysis was performed using QStar XL Hybrid ESI Quadrupole Time-of Flight Mass Spectrometer, ESI-qQ-TOF-MS/MS (AB SCIEX™; MDS-SCIEX, Concord, Ontario, Canada). Samples were resuspended in RPLC buffer C (3% ACN and 0.1% TFA), injected and captured onto a 0.3 × 5 mm pre-analytical trap cartridge (5 μm C18 columns) (Thermo Scientific). Peptides were subsequently eluted using an automated gradient with a flow rate of 0.3 μl/min. Online nLC was achieved using a 150 min binary gradient with RPLC buffer A (0.1% formic acid and 3% ACN), and RPLC buffer B (0.1% formic acid and 97% ACN). A programmed gradient started with a 20 min linear ramp from 0 to 3% buffer B, 95 min ramp from 3 to 35% buffer B, a 30 s rapid ramp up to 90% buffer B, 6.5 min isocratic wash 90% buffer B, 30 s rapid ramp down to 3% buffer B, followed by 27.5 min isocratic wash 3% buffer B. Data acquisition in the mass spectrometer was set to acquire in the positive ion mode, with the precursor ion scan performed within a range of 330–2000 *m/z* and a selected mass detector range of 400–1250 *m/z*, on a predefined accumulation time of 1 s (AnalystQS Software, AB SCIEX™). During the TOF-MS scan, two dynamically selected precursors with a +2 or +3 charge state were isolated for CID fragmentation. Samples were reanalyzed on a second LC–MS injection with identical parameters to increase sample coverage [24].

2.10. *MS data analysis*

Peak list conversion was performed using the mascot.dll embedded script (V1.6) coupled with Analyst QS 1.1.1 (AB SCIEX™) with MS/MS group summations and the iTRAQ region deisotoping removed. Protein identification and quantification was carried out in Phenyx v2.6 (GeneBio S.A., Geneva, Switzerland), using a database comprising all *Cyanothece* sp. CCY 0110 protein sequences obtained from UniProt (6413 entries retrieved, March 2014). General search parameters allowed for MS and MS/MS tolerance up to 0.1 Da and one missed cleavage. Fixed protein modifications included iTRAQ lysine and iTRAQ N-terminus (+304 Da) and methyl-thiol of cysteins (+46 Da), and the oxidation of methionine (+16 Da) was defined as variable modification. Acceptance threshold for peptide identification was set at peptide length ≥6, z-score ≥5 and p-value ≤1 e − 4. False discovery rate (FDR) was calculated using a decoy database automatically created by reversing the sequences from the target database, and only proteins satisfying a 1% FDR and identified with at least two peptides unique were considered for further quantitative analysis. iTRAQ

labeling efficiency was calculated using peptide data where iTRAQ lysine and iTRAQ N-terminus (+304 Da) modifications were set as variable instead of fixed, and was 95.1% and 95.9% for the copper and cadmium data sets respectively. Since iTRAQ ratios and determination of proteins altered between samples, it was carried out an in house data analysis pipeline [25] by which protein quantifications were obtained by computing the geometric means of the reporters' intensities. Median correction was subsequently applied to every reporter in order to compensate for systematic errors. These factors, estimated at the protein level, are used in subsequent analysis. The reporters' intensities, in each individual MS/MS scan, were then themselves median corrected using the same factors. Since two replicates are available for each condition, a change is reported only if it is significant regardless of which replicate is chosen to perform the *t* test comparison. Proteins were subsequently organized into functional groups according to their Gene Ontology information available in Uniprot (http://www.uniprot.org/).

2.11. Quantification of RbcL and PsaC by Western blot analysis

The relative abundances of the large subunit of ribulose-1,5-bisphosphate carboxylase/oxygenase (RuBisCo) — RbcL and the photosystem I (PSI) protein PsaC were determined by Western blot analysis as described previously [26] using 3 biological replicates and 3 technical replicates, and using the same protein extracts as for the iTRAQ assays. The primary antibodies used were rabbit polyclonal antibody anti-RbcL at a 1:5000 dilution (RuBisCo Quantification Kit, Agrisera Antibodies, Vännäs, Sweden) and anti-PsaC at a 1:1000 dilution (Agrisera Antibodies), and the secondary antibody was goat anti-rat immunoglobulin G linked to horseradish peroxidase (Amersham Biosciences, Buckinghamshire, UK) at a 1:5000 dilution. Blot images were acquired using the ChemiDoc™ XRS$^+$ System and analyzed using the Image Lab™ software (Bio-Rad Laboratories).

2.12. In vivo detection of ROS production

4 ml of cultures (3 biological replicates) grown in the same conditions as the ones used for iTRAQ assays, were incubated with 4 μL of 2′,7′-dichlorofluorescein diacetate (H2DCF-DA; Molecular Probes, Inc., Eugene, OR, USA) for 1 h in the dark at 30 °C. Stock solution contains 5 mM (w/v) of H2DCF-DA in 100% DMSO and was kept at −20 °C. The fluorescence of the samples was measured by a spectrofluorometer (FluoroMax-4®, Horiba Scientific, Japan) with an excitation wavelength of 485 nm and emission wavelengths between 500 nm and 600 nm, at 30 °C.

2.13. Superoxide dismutase (SOD) activity measurements

Proteins extracts (3 biological replicates) from cell grown in the same conditions as for iTRAQ assays were obtained using 50 mM phosphate buffer pH 6.8 supplemented with protease inhibitor cocktail (Roche Diagnostics GmbH, Penzberg, Germany). Extraction and quantification were performed as described above. SOD gel zymography was performed as described previously [23]. Gel images were acquired using the GS-800™ Calibrated densitometer and analyzed using the Quantity One® 1-D analysis software (Bio-Rad Laboratories).

2.14. O_2 evolution measurements

For the O_2 evolution measurements the cells were grown in the same conditions as for the iTRAQ experiments and O_2 evolution was measured using a Clark type O_2 electrode (Oxygraph, Hansatech Ltd., Norfold, UK). The calibration was performed using sodium bisulfite and air saturated water at 30 °C. Assays were carried out using 1 ml of culture under a continuous irradiance of 50 μE/m^2/s. A magnetic stirrer operating at 100 rpm was used to obtain a homogeneous suspension and the temperature of the chamber was kept at 30 °C. Protein content was determined using the Lowry method [27], and the rates of O_2 evolution were expressed as nmol O_2/ min/ mg protein.

2.15. Statistical analysis

Data obtained in Western blots, in vivo detection of ROS production, gel zymography and O_2 evolution measurements were statistically analyzed in GraphPad Prism v6 (GraphPad Software, Inc., San Diego, CA, USA) using a one-way analysis of variance (ANOVA), followed by a Tukey's multiple comparison with a confidence level of 95% ($\alpha = 0.05$). To investigate the groups of proteins with similar variation of its relative levels in the different phenotypes, a hierarchical cluster analysis was performed. For that, protein ratios were transformed into ordinal/ranked variables according to their values, namely: 0 — significant fold change < 1, 1 — no significant fold change, 2 — significant fold change > 1 and clustered using the "Centroid Linkage" method and the "Squared Euclidean Distance" measure. The cluster analysis was performed using the IBM® SPSS® Statistics 20.0 (IBM, Armonk, NY, USA).

3. Results

3.1. Effects of different metals/metal concentrations in growth and EPS production by *Cyanothece* cells

To obtain a holistic perspective of the strategies (including short- and long-term mechanisms) triggered by the cells to decrease the toxic effects of different metals, different concentrations and exposure times were assessed. For this purpose, the effects of mono- (Li^+) and divalent cations (Cu^{2+}, Pb^{2+}, Cd^{2+}) on the growth/survival of *Cyanothece* cells and EPS production were evaluated. Standard high purity metal solutions were used and the cultures were buffered to maintain neutral pH throughout the experiments (for details see Material and methods). The growth was monitored measuring the OD and chlorophyll *a* content, and the data obtained revealed linear growth patterns. As anticipated, cell growth was negatively affected by the presence of the metals, with increasing concentrations leading to a corresponding decrease in growth rate and maximum OD obtained. Concerning the chronic exposure (up to 1 month), cells were more affected by Cu^{2+} (with 0.2 mg/l leading to cell death), followed by Pb^{2+} (10 mg/l), Cd^{2+} (10 mg/l) and Li^+ (70 mg/l); see Fig. 2 and Supplementary Fig. 1. When the cells were exposed to 0.1 mg/l of Cu^{2+}, the decrease in growth was more

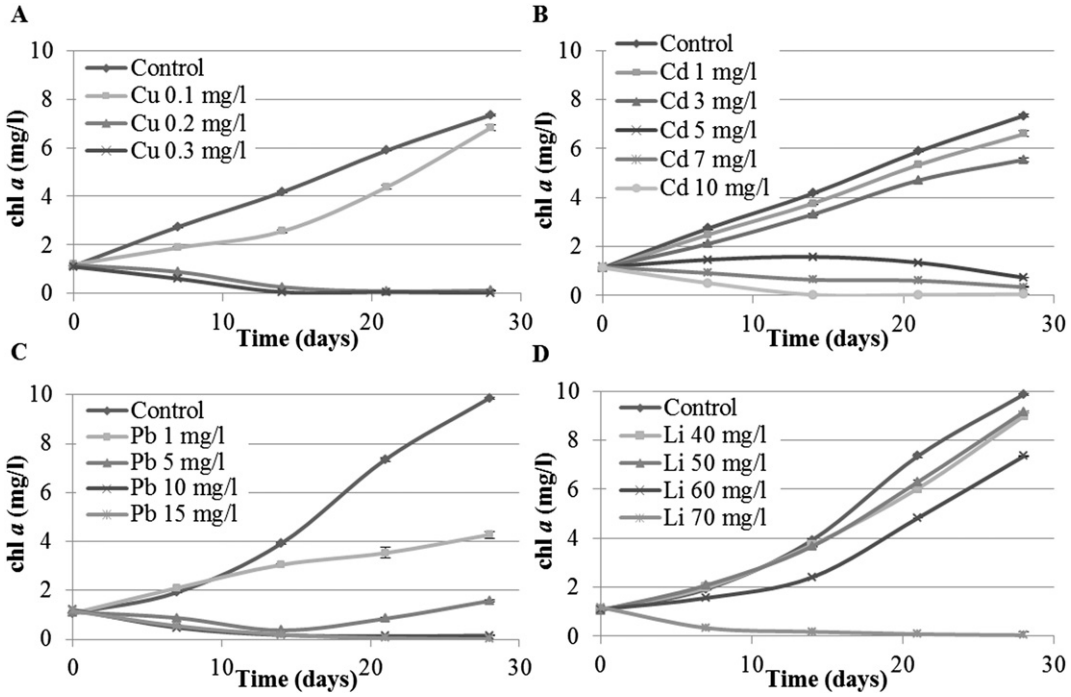

Fig. 2 – Effects of different metals/metal concentration on *Cyanothece* sp. CCY 0110 growth. Cells were cultured in ASNIII buffered medium or the same medium supplemented with different concentrations of copper (A), cadmium (B), lead (C) or lithium (D), under a 12 h light (50 μE/m^2/s)/12 h dark regimen, at 30 °C and orbital shaking at 150 rpm. Results are expressed in mg of chlorophyll *a* per liter of culture. Data are means ± standard deviations (*n* = 3).

pronounced in first 10 days of culture with a clear recovery observed afterwards (this pattern was always observed for this sub-lethal concentration). For practical reasons, the effects of acute exposure were only assessed for one essential metal (Cu^{2+}) and one non-essential metal (Cd^{2+}). For this purpose, *Cyanothece* cells were grown for 9 days in ASNIII buffered medium, before adding 10 times the sub-lethal metal concentrations: 1 mg/l of Cu^{2+} or 50 mg/l of Cd^{2+}. After 24 h, the decrease in growth (chlorophyll *a* content) for the cultures supplemented with Cu^{2+} and Cd^{2+} respectively, was 6.4% and 13.7% compared to the control, continuing to decline progressively after that (data not shown). In general, total carbohydrates and RPS production followed the pattern of growth (data not shown), with the RPS production reaching a maximum of 258 mg/l in the control conditions (without added metal) and constituting in average 58 ± 6% of the total carbohydrates in all cultures tested (with or without metal).

3.2. *Ultrastructural changes and elemental composition analysis*

TEM–EDX analyses were performed in order to observe ultrastructural changes and to identify possible sites of metal accumulation inside the cells. In the presence of sub-lethal concentrations of any of the four metals tested, significant ultrastructural changes were observed at 10, 20 and 30 days of culture, particularly in the presence of Cd^{2+} and Li^{+}. For parsimony reasons, only images of cells collected after 30 days are shown in Fig. 3A-E (other results in Supplementary Fig. 2). The ultrastructural changes are mainly related to the thylakoids, with disorganization and disintegration of thylakoid membranes and increase of the intrathylakoidal space. In addition, the occurrence of inclusions was also observed. After 24 h acute exposure, the effects of Cd^{2+} are similar to those observed for chronic exposure (Fig. 3G), while the ultrastructure of the cells exposed to 1 mg/l of Cu^{2+} is altered overall (Fig. 3F). No obvious intracellular sequestration of the metals was detected by EDX spectroscopy. However, several differences can be observed by comparison of the elemental composition of the cells grown in the absence or in the presence of each metal (Fig. 4). In general, these differences were consistent in the four different areas of the cells chosen to perform this analysis, namely outer membrane, cytoplasm, thylakoids and inclusions. Carbon, oxygen and nitrogen were, as expected, the main elements observed, but also nine micro-elements (Na, Mg, Al, P, S, Cl, Ca, Fe and Cu) were detected. Overall, a higher percentage of micro-elements was detected in the cells grown in the presence of metal ions. In particular, in those grown in the presence of Li^{+} increased percentages of magnesium, aluminum, sulfur and calcium were observed (Li^{+} itself could not be detected by the technique used due to its single electron valence).

Furthermore, the amount of metals in the supernatant was evaluated by atomic absorption spectroscopy (data not shown). The results obtained showed that for chronic exposure and Cd^{2+} acute exposure most of the metals are found in the supernatant, while for Cu^{2+} acute exposure only half of the amount is found in the supernatant.

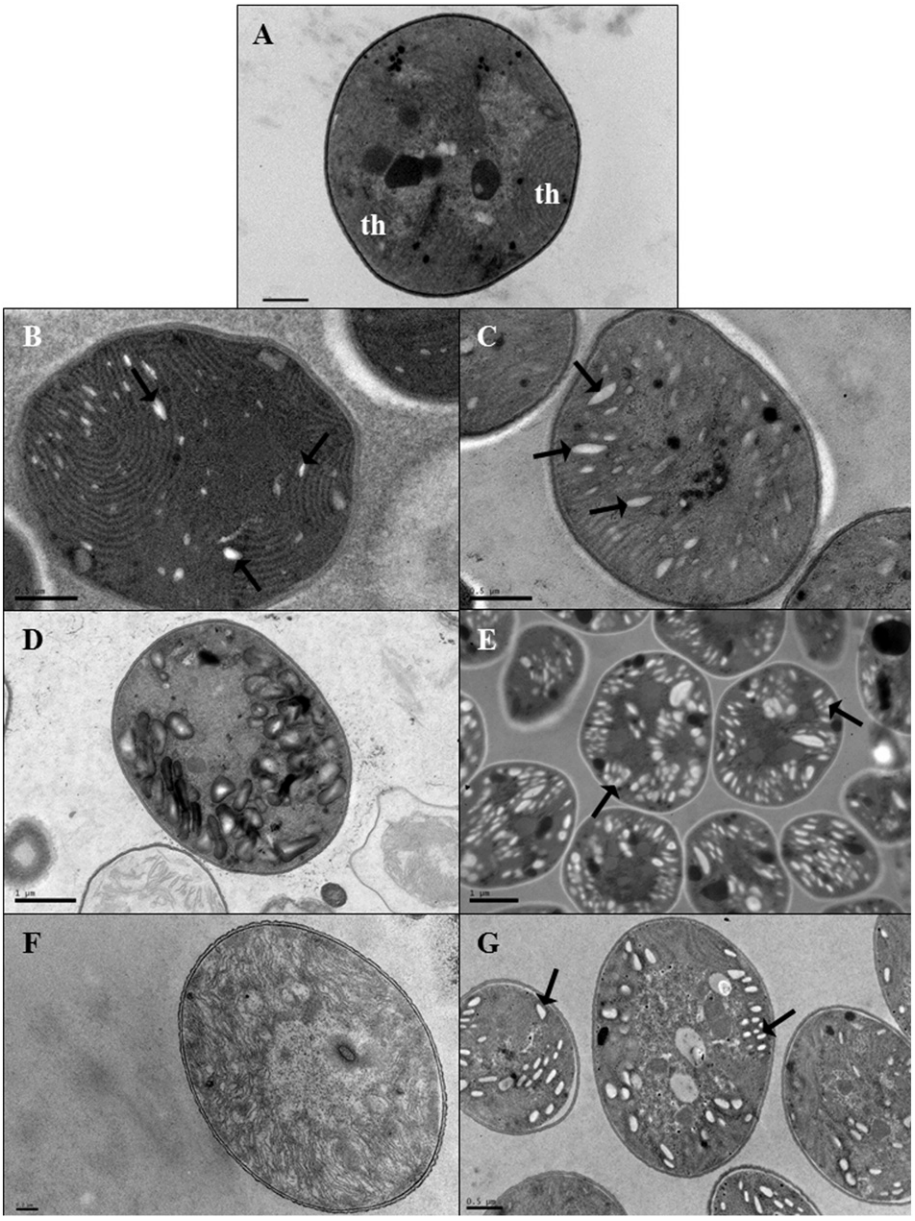

Fig. 3 – Transmission electron micrographs of *Cyanothece* sp. CCY 0110 grown in the absence/presence of different metals. Cells were grown in ASNIII buffered medium (control) (A), or medium supplemented with sub-lethal concentrations of copper (0.1 mg/l) (B), lead (1 mg/l) (C), cadmium (5 mg/l) (D) or of lithium (60 mg/l) (E) for 30 days, or copper (1 mg/l) (F) or cadmium (50 mg/l) (G) for 24 h, under a 12 h light (50 μE/m^2/s)/12 h dark regimen, at 30 °C and orbital shaking at 150 rpm. th — thylakoids, arrows indicate altered intrathylakoidal spaces. Scale bars: (A–C, G) = 0.5 μm; (D–E) = 1 μm; (F) = 0.2 μm.

3.3. Proteomes of Cyanothece grown in the absence/presence of metals

To evaluate, at the molecular level, the putative effects of chronic (sub-lethal metal concentrations for 10 or 20 days) and acute (10 times the sub-lethal metal concentration for 24 h) exposure to an essential and a non-essential metal, two independent 8-plex iTRAQ studies were performed, one for Cu^{2+} (iTRAQ study 1) and another for Cd^{2+} (iTRAQ study 2). Using the stringent criteria defined in the Material and methods, 202 (98 with two or more peptides) and 268 (130 with two or more peptides) proteins were identified and quantified for studies 1 and 2, respectively. Detailed information is provided in Mota et al. [28].

To identify relatively homogeneous groups of proteins (clusters) with similar variation patterns, hierarchical cluster analyses were performed. The strength of the analyses performed was improved by including all the possible comparisons/ratios (Fig. 1), which minimizes the effects of over- or underestimated ratios and increases confidence. For each iTRAQ study, 6 statistically supported protein clusters (A–F) were formed (Fig. 5; [28]). Regarding study 1, 80% of proteins was included in cluster A1 (no significant change in any of the conditions tested), cluster B1 (no significant change

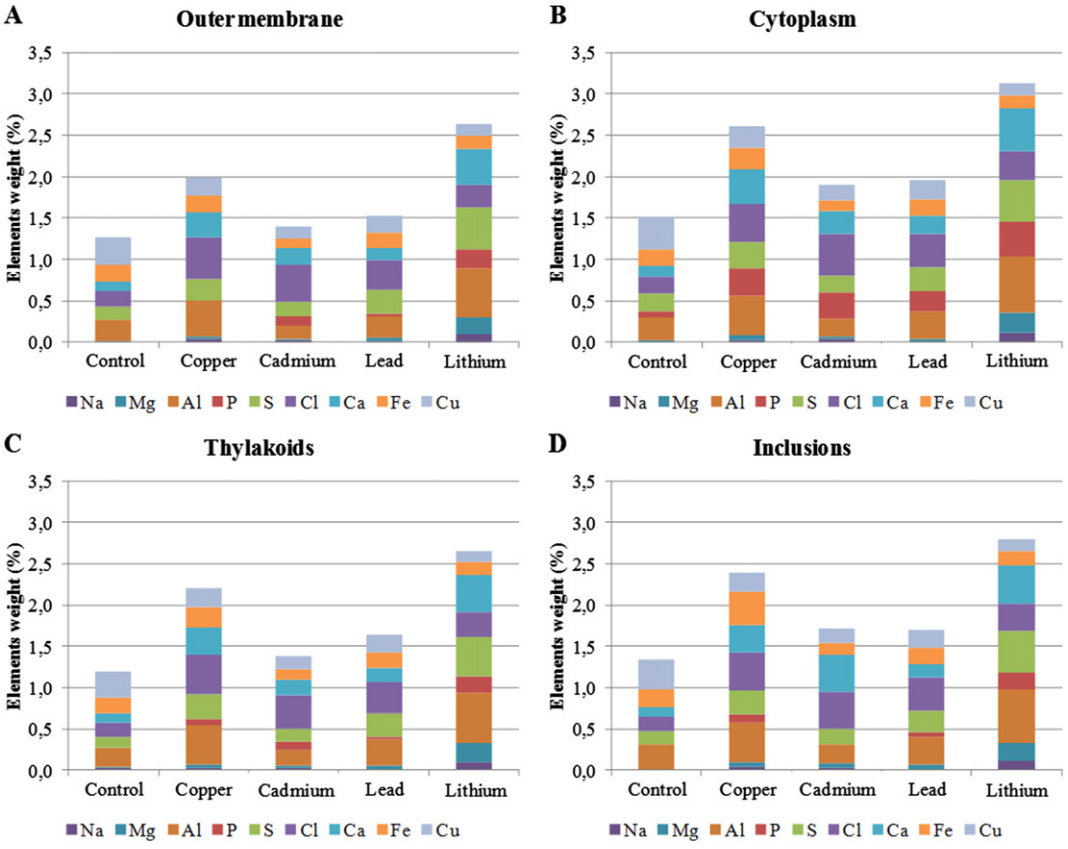

Fig. 4 – Energy dispersive X-ray (EDX) spectroscopy of *Cyanothece* sp. CCY 0110. Weight percentage of micro-elements detected in four different areas of *Cyanothece* cells: outer membrane (A), cytoplasm (B), thylakoids (C) and inclusions (D). Cells were grown 30 days in ASNIII buffered medium (control) or the same medium supplemented with sub-lethal concentrations of copper (0.1 mg/l), lead (1 mg/l), cadmium (5 mg/l) or lithium (60 mg/l), with a 12 h light (50 μE/m^2/s)/12 h dark regimen, 30 °C and orbital shaking at 150 rpm.

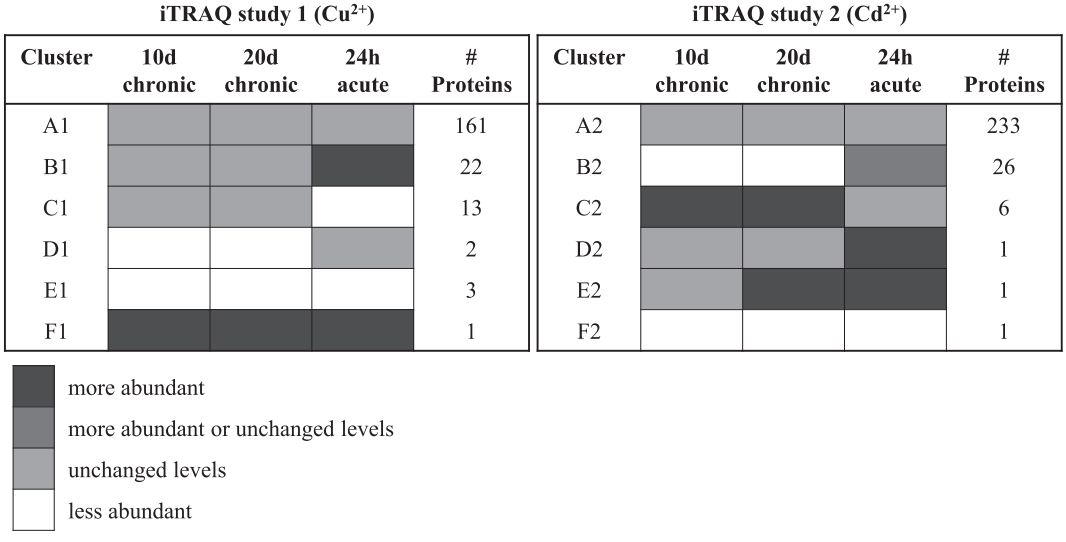

Fig. 5 – Hierarchical cluster analysis of the proteins quantified in iTRAQ study 1 (Cu^{2+} exposure) and iTRAQ study 2 (Cd^{2+} exposure). Six (A–F) clusters of proteins were defined according to the variation of their relative levels in *Cyanothece* cells grown in ASNIII buffered medium supplemented with 0.1 mg/l of Cu^{2+} or 5 mg/l of Cd^{2+} (for 10 or 20 days, chronic exposure) or 1 mg/l of Cu^{2+} or 50 mg/l of Cd^{2+} (24 h, acute exposure). The number of proteins in each cluster is indicated in the right columns. Clusters were calculated using all ratios to minimize over- or underestimations. Data were converted into ordinal/ranked variables and clustered using the "centroid linkage" method and the "squared Euclidean distance" measure.

in 10 and 20 days chronic exposure, and higher abundance in acute exposure) and cluster C1 (no significant change in 10 and 20 days chronic exposure, and lower abundance in acute exposure). Overall, the acute exposure was the condition that promoted more quantitative proteome changes — 19%. Concerning study 2, 87% of the proteins were found in cluster A2 (no change in any of the conditions) and cluster B2 (lower abundance in 10 and 20 days chronic exposure). A number of proteins were also grouped in cluster C2 (higher abundance in 10 and 20 days chronic exposure). In contrast with what was observed for Cu^{2+}, in study 2 — Cd^{2+}, the 10 and 20 days chronic exposure were the conditions that caused more differential protein expression, 12% and 13% respectively.

To gain insight into the biological significance of the changes observed, the proteins were grouped according to their annotated function and the Gene Ontology information. The majority of the proteins with known functions were associated with photosynthesis, CO_2 fixation and carbohydrate metabolism, translation, and nitrogen and amino acid metabolism (Figs. 6A and 7A, Table 1). Nevertheless, 27% and 24% of the proteins identified/quantified for studies 1 and 2 respectively, remain uncharacterized. It was also observed that, within each functional category, the number of differentially expressed proteins in metal-exposed cells compared to the control were different in iTRAQ study 1 — Cu^{2+} exposure and iTRAQ study 2 — Cd^{2+} exposure (Figs. 6B and 7B).

Several proteins involved in photosynthesis were reliably identified and quantified (Table 1; [28]). The levels of PSI and PSII components were differentially affected by the metals tested, generally increasing in cells after acute Cu^{2+} exposure

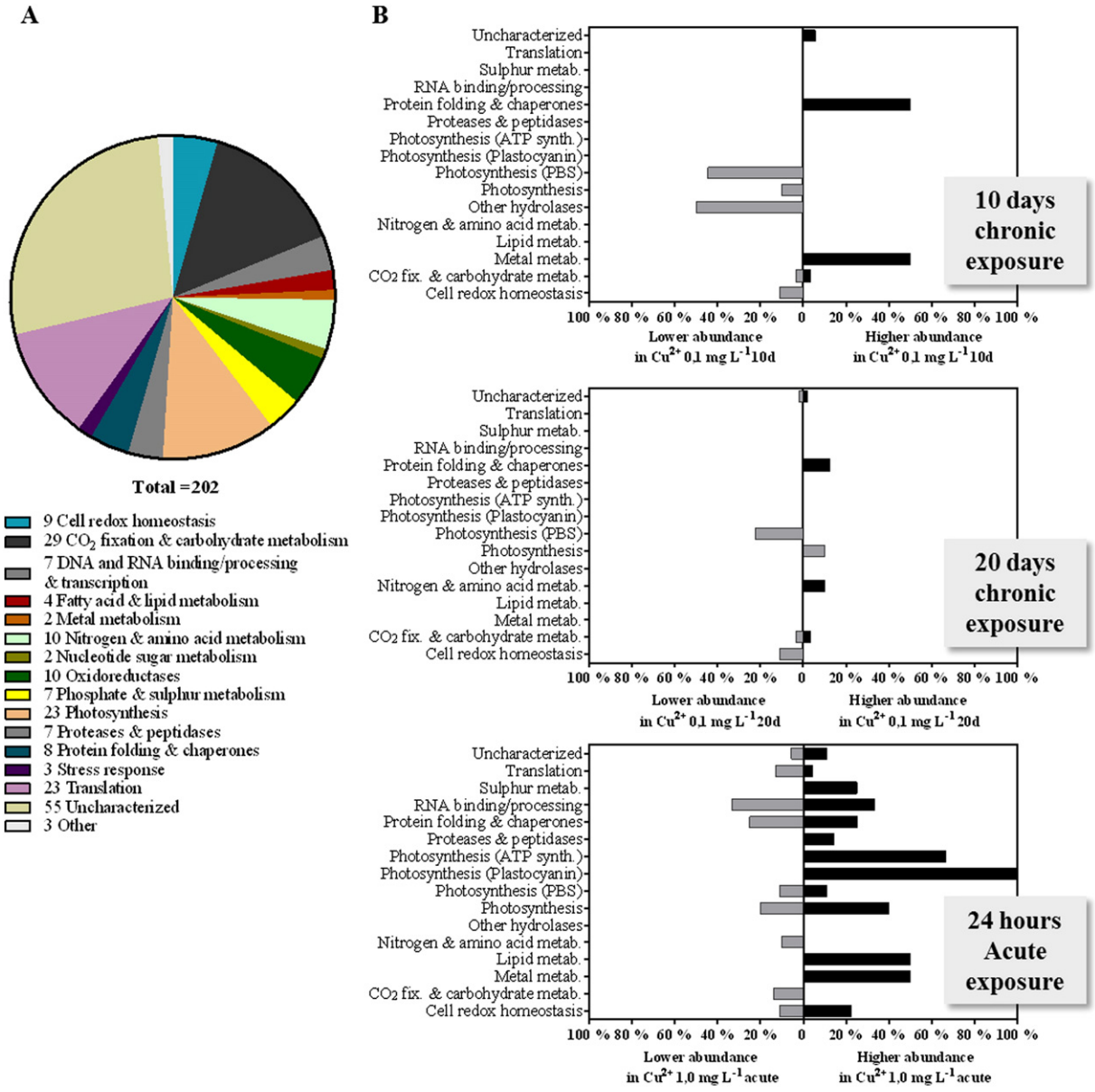

Fig. 6 – Distribution and fold changes of proteins identified and quantified in iTRAQ study 1 (Cu^{2+} exposure). (A) Distribution by functional groups — the total number of proteins and the number in each group is indicated. (B) Percentage of proteins with significant fold changes in each functional category compared to the control (no metal supplementation).

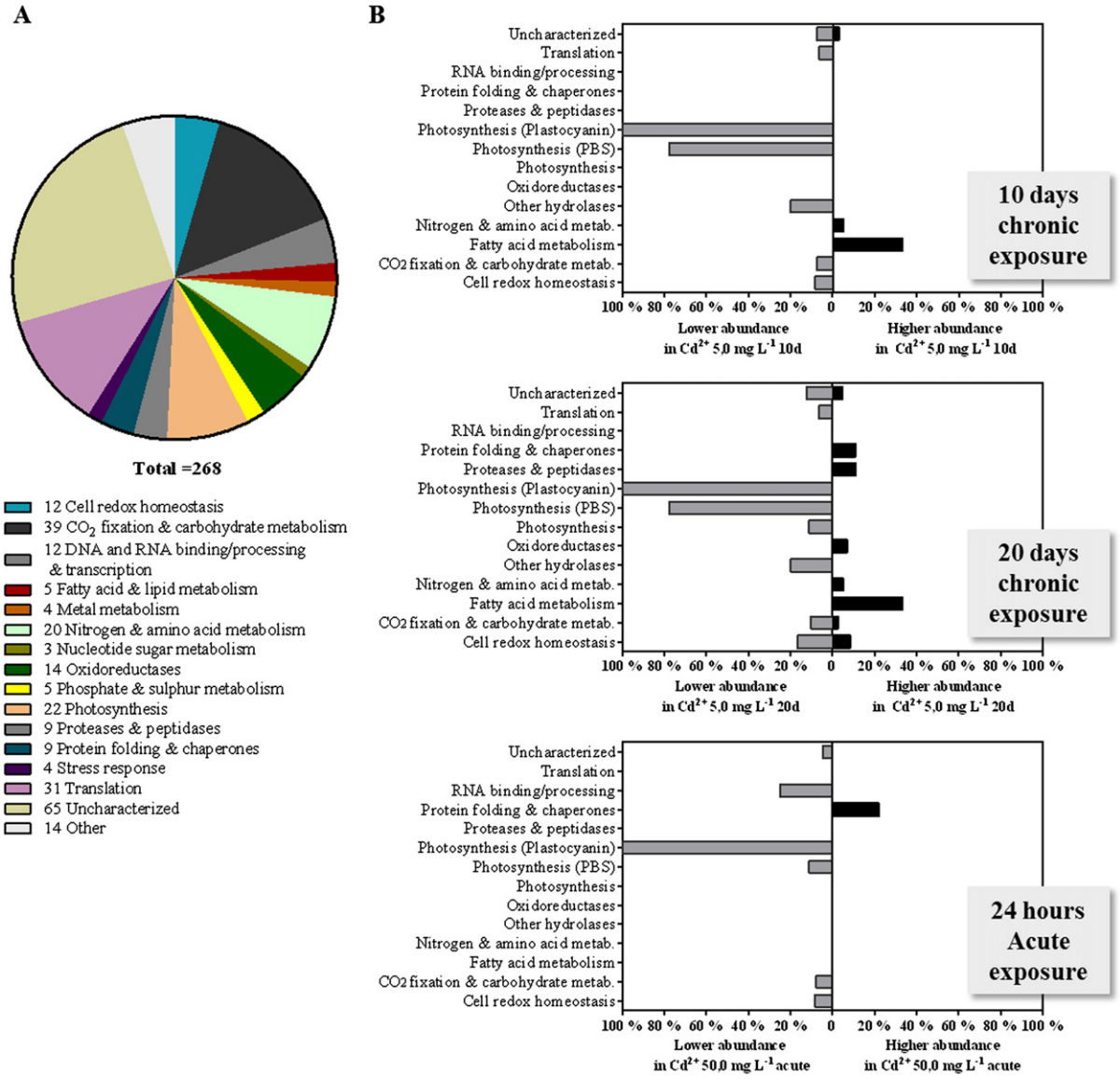

Fig. 7 – Distribution and fold changes of proteins identified and quantified in iTRAQ study 2 (Cd^{2+} exposure). (A) Distribution by functional groups — the total number of proteins and the number in each group is indicated. (B) Percentage of proteins with significant fold changes in each functional category compared to the control (no metal supplementation).

(cluster B1) and remaining constant in all Cd^{2+}-exposed phenotypes (cluster A2). Likewise, the levels of the components of the phycobilisomes (PBS) were also differentially affected, but in this case did not change significantly when the cells were exposed to Cu^{2+} (most grouped in cluster A1, even though the levels of some components were lower after 10 and 20 days chronic exposure, clusters C1 and D1), and generally decreased in Cd^{2+} chronic exposure conditions (cluster B2). Interestingly, for ATP synthase, the levels of the alpha and beta subunits responded to Cu^{2+} metal stress, increasing in acute exposure. In contrast, the ferredoxin-NADP reductase (FNR) followed a converse pattern, decreasing in Cu^{2+} exposure and Cd^{2+} at 20 days chronic exposure. Concerning plastocyanin, the levels increased in acute Cu^{2+} exposure and decreased in all Cd^{2+} stress conditions.

In agreement with that observed for the photosynthesis related proteins, the levels of enzymes involved in CO_2 fixation and carbohydrate metabolism were also differentially affected by Cu^{2+} and Cd^{2+}. The levels of the large subunit of RuBisCo (RbcL) decreased in Cu^{2+}-exposed cells, as well as in 20 days chronic Cd^{2+} stress. Considering the glycolytic enzymes, one glyceraldehyde-3-phosphate dehydrogenase and the phosphoglycerate kinase decreased in acute Cu^{2+}-exposed cells, whereas the phosphoglucomutase levels increased in chronic conditions. The levels of the later enzyme also decreased in Cd^{2+}-exposed cultures. On the other hand, the levels of fructose-bisphosphate aldolase and sodium-dependent bicarbonate transporter decreased in all Cd^{2+} stress conditions.

Table 1 – List of quantified proteins obtained for iTRAQ studies 1 and 2 and discussed in this work [a].

Gene name/locus tag	Uniprot ID [b]	Protein (gene product) [c]	iTRAQ study 1 (Cu^{2+} exposure)				iTRAQ study 2 (Cd^{2+} exposure)			
			10d/ control	20d/ control	Acute/ control	Cluster [d]	10d/ control	20d/ control	Acute/ control	Cluster [d]
Photosynthesis										
CY0110_18357	A3IJ03	Phycocyanin a subunit	1.00	1.00	1.00	A1	0.38	0.21	0.58	B2
CY0110_18322	A3IIZ6	Phycocyanin b subunit	1.00	1.00	1.88	B1	0.47	0.30	1.00	B2
CY0110_18472	A3IJ26	Phycocyanin associated linker protein	1.00	1.00	1.00	A1	1.00	1.00	1.00	A2
CY0110_24111	A3ILQ6	Phycobilisome core component	1.00	1.00	1.00	A1	1.00	1.00	1.00	A2
CY0110_24691	A3IMR4	Phycobilisome LCM core-membrane linker polypeptide	0.34	0.32	1.00	D1	0.24	0.11	1.00	B2
CY0110_04066	A3IT83	Phycobilisome rod-core linker polypeptide CpcG	0.36	0.47	1.00	D1	0.48	0.23	1.00	B2
CY0110_24151	A3ILR4	Allophycocyanin-B	0.51	1.00	0.34	C1	0.48	0.41	1.00	B2
CY0110_30568	A3ITK1	Allophycocyanin b chain	0.45	1.00	1.00	A1	0.61	0.48	1.00	B2
CY0110_30573	A3ITK2	Allophycocyanin a chain	1.00	1.00	1.00	A1	0.41	0.21	1.00	B2
CY0110_10187	A3IGZ4	Photosystem I subunit II	1.00	1.00	1.00	A1	1.00	1.00	1.00	A2
CY0110_05462	A3IQ52	Photosystem I subunit III	1.00	1.00	4.12	B1	1.00	1.00	1.00	A2
psaC CY0110_30091	A3IRR7	Photosystem I iron-sulfur center (EC 1.97.1.12) (9 kDa polypeptide) (PSI-C) (Photosystem I subunit VII) (PsaC)	1.00	1.00	9.58	B1	1.00	1.00	1.00	A2
psaA CY0110_22961	A3IYL1	Photosystem I P700 chlorophyll a apoprotein A1 (EC 1.97.1.12) (PsaA)	1.00	1.00	2.75	B1	1.00	1.00	1.00	A2
CY0110_27670	A3IR74	Photosystem I reaction center protein subunit XI	1.00	1.00	1.00	A1				
psbU CY0110_00665	A3INE8	Photosystem II 12 kDa extrinsic protein (PS II complex 12 kDa extrinsic protein) (PSII-U)	1.00	1.00	1.94	B1	1.00	1.00	1.00	A2
CY0110_14033	A3IUE0	Photosystem II manganese-stabilizing polypeptide	1.00	1.00	1.00	A1	1.00	1.00	1.00	A2
CY0110_00055	A3IN26	Ferredoxin, 2Fe–2S	1.00	1.00	0.23	C1	1.00	1.00	1.00	A2
CY0110_28804	A3ISY1	Ferredoxin–NADP reductase (EC 1.18.1.2)	0.45	0.11	0.04	E1	1.00	0.41	1.00	B2
petA CY0110_29464	A3INI8	Apocytochrome f	1.00	1.00	1.00	A1				
CY0110_28324	A3IMH3	Plastocyanin	1.00	1.00	2.41	B1	0.30	0.28	0.35	B2
atpA CY0110_17952	A3IIS2	ATP synthase subunit alpha (EC 3.6.3.14) (ATP synthase F1 sector subunit alpha) (F-ATPase subunit alpha)	1.00	1.00	2.22	B1	1.00	1.00	1.00	A2
atpD atpB CY0110_22292	A3IL04	ATP synthase subunit beta (EC 3.6.3.14) (ATP synthase F1 sector subunit beta) (F-ATPase subunit beta)	1.00	1.00	1.75	B1	1.00	1.00	1.00	A2
atpC CY0110_22287	A3IL03	ATP synthase epsilon chain (ATP synthase F1 sector epsilon subunit) (F-ATPase epsilon subunit)	1.00	1.00	1.00	A1	1.00	1.00	1.00	A2
CO_2 fixation and carbohydrate metabolism										
rbcL cbbL CY0110_00450	A3INA5	Ribulose bisphosphate carboxylase large chain (RuBisCO large subunit) (EC 4.1.1.39)	0.47	0.43	0.32	E1	1.00	0.39	1.00	B2
CY0110_13067	A3IQZ4	Fructose-bisphosphate aldolase	1.00	1.00	1.00	A1	0.49	0.35	0.54	B2
pgk CY0110_12707	A3IQS2	Phosphoglycerate kinase (EC 2.7.2.3)	1.00	1.00	0.16	C1	0.39	0.43	0.51	B2

(continued on next page)

Table 1 (*continued*)

Gene name/locus tag	Uniprot ID[b]	Protein (gene product)[c]	iTRAQ study 1 (Cu^{2+} exposure)				iTRAQ study 2 (Cd^{2+} exposure)			
			10d/ control	20d/ control	Acute/ control	Cluster[d]	10d/ control	20d/ control	Acute/ control	Cluster[d]
CO_2 fixation and carbohydrate metabolism										
CY0110_08156	A3ISB6	Glyceraldehyde-3-phosphate dehydrogenase (EC 1.2.1.12)	1.00	1.00	0.25	C1	1.00	1.00	1.00	A2
CY0110_24626	A3IMQ1	Phosphoglucomutase (EC 5.4.2.2)	1.50	1.39	1.00	A1	1.00	1.00	1.00	A2
CY0110_13751	A3IPU9	Sodium-dependent bicarbonate transporter	1.00	1.00	1.00	A1	0.36	0.11	0.15	B2
Nitrogen fixation and amino acid metabolism										
CY0110_09196	A3IVG2	Glutamine synthetase (EC 6.3.1.2)	1.00	1.00	1.00	A1	1.77	2.75	1.00	C2
Nucleotide sugar metabolism										
ndk CY0110_09525	A3IYQ9	Nucleoside diphosphate kinase (NDK) (NDP kinase) (EC 2.7.4.6) (Nucleoside-2-P kinase)	1.00	1.00	1.00	A1	1.00	1.00	1.00	A2
CY0110_10752	A3IHA7	UDP-glucose/GDP-mannose dehydrogenase	1.00	1.00	1.00	A1				
CY0110_09992	A3IGV5	3-beta hydroxysteroid dehydrogenase/isomerase					1.00	1.00	1.00	A2
CY0110_07744	A3IP34	Perosamine synthetase					1.00	1.00	1.00	A2
Protein folding and chaperones										
groL groEL CY0110_17702	A3IIM2	60 kDa chaperonin (GroEL protein) (Protein Cpn60)	1.35	1.00	0.36	C1	1.00	1.00	1.00	A2
groL groEL CY0110_06524	A3IYB7	60 kDa chaperonin (GroEL protein) (Protein Cpn60)	1.52	1.00	0.39	C1	1.00	1.22	1.53	E2
groS groES CY0110_06529	A3IYB8	10 kDa chaperonin (GroES protein) (Protein Cpn10)	2.74	1.45	7.18	F1	1.00	1.00	1.00	A2
dnaK CY0110_25571	A3IRL4	Chaperone protein DnaK (HSP70) (Heat shock 70 kDa protein) (Heat shock protein 70)	1.34	1.00	1.00	A1	1.00	1.00	1.33	D2
Cell redox homeostasis										
CY0110_00265	A3IN68	Superoxide dismutase (EC 1.15.1.1)	1.00	1.00	2.64	B1	1.00	1.00	1.00	A2
katG CY0110_25833	A3IP51	Catalase-peroxidase (CP) (EC 1.11.1.21) (Peroxidase/catalase)					1.00	1.00	1.00	A2
CY0110_05412	A3IQ42	Ferritin and Dps	1.00	1.00	1.00	A1	1.00	1.25	1.00	A2
CY0110_08886	A3IW63	Ferritin and Dps	1.00	1.00	1.00	A1	1.00	0.40	1.00	B2
CY0110_08866	A3IW59	Thioredoxin	1.00	1.00	1.00	A1	1.00	1.00	1.00	A2
CY0110_08601	A3IZ92	Thioredoxin	1.00	1.00	3.84	B1	1.00	1.00	1.00	A2
CY0110_06889	A3IZ81	Rehydrin	0.47	0.29	0.14	E1	0.37	0.40	0.23	F2
Sulfur metabolism										
CY0110_16477	A3IHX7	Arylsulfatase	1.00	1.00	2.31	B1	1.00	1.00	1.00	A2
sat CY0110_15470	A3IWF9	Sulfate adenylyltransferase (EC 2.7.7.4) (ATP-sulfurylase) (sulfate adenylate transferase)	1.00	1.00	1.00	A1	1.00	1.00	1.00	A2
CY0110_10897	A3IZG7	Sulfite reductase, ferredoxin dependent	1.00	1.00	1.00	A1	1.00	1.00	1.00	A2
CY0110_02919	A3IJZ7	Sulfatase	1.00	1.00	1.00	A1				
Metal-related metabolism										
CY0110_13696	A3IPT8	Iron transport protein	1.00	1.00	4.20	B1	1.00	1.00	1.00	A2
CY0110_10262	A3IH09	Uncharacterized protein	1.71	1.00	1.00	A1	1.00	1.00	1.00	A2
CY0110_02244	A3IM52	Arsenate reductase					1.00	1.00	1.00	A2
CY0110_00210	A3IN57	Molybdopterin converting factor, subunit 2					1.00	1.00	1.00	A2

Table 1 (*continued*)

Gene name/locus tag	Uniprot ID[b]	Protein (gene product)[c]	iTRAQ study 1 (Cu^{2+} exposure)				iTRAQ study 2 (Cd^{2+} exposure)			
			10d/ control	20d/ control	Acute/ control	Cluster[d]	10d/ control	20d/ control	Acute/ control	Cluster[d]
Fatty acid metabolism										
CY0110_09076	A3IVD8	Long-chain-fatty-acid CoA ligase					1.63	3.07	1.00	C2
Translation										
rplW rpl23 CY0110_05227	A3IQ05	50S ribosomal protein L23	1.00	1.00	1.00	A1	0.48	0.44	1.00	B2
rplL rpl12 CY0110_09111	A3IVE5	50S ribosomal protein L7/L12	1.00	1.00	2.18	B1	0.44	0.37	1.00	B2
rplA rpl1 CY0110_09121	A3IVE7	50S ribosomal protein L1	1.00	1.00	0.17	C1	1.00	1.00	1.00	A2
tsf CY0110_00220	A3IN59	Elongation factor Ts (EF-Ts)	1.00	1.00	0.14	A1	1.00	1.00	1.00	A2
fusA CY0110_20113	A3ISG8	Elongation factor G (EF-G)	1.00	1.00	0.24	C1	1.00	1.00	1.00	A2
Uncharacterized										
CY0110_09677	A3IGP2	Uncharacterized protein	1.00	1.00	1.00	A1	1.00	0.25	1.00	B2
CY0110_10307	A3IH18	Uncharacterized protein	3.14	1.00	1.00	A1	1.00	1.00	1.00	A2
CY0110_17517	A3III5	Uncharacterized protein	2.19	1.53	1.00	A1	1.00	1.00	1.00	A2
CY0110_23344	A3IMW3	Uncharacterized protein	1.00	1.00	1.00	A1	3.24	3.97	1.00	C2
CY0110_13346	A3IPL8	Uncharacterized protein	1.00	1.00	1.00	A1	1.00	1.87	1.00	C2
CY0110_13741	A3IPU7	Uncharacterized protein	1.00	1.00	1.00	A1	1.00	0.30	0.47	B2
CY0110_05392	A3IQ38	Uncharacterized protein	1.00	1.00	1.00	A1	1.00	1.60	1.00	C2
CY0110_11437	A3IQF8	Rhodanese-like protein	1.34	1.00	1.38	A1	1.00	1.00	1.00	A2
CY0110_11522	A3IQH5	Uncharacterized protein	1.00	1.00	1.00	A1	0.54	0.65	1.00	B2
CY0110_21040	A3IRB2	Uncharacterized protein	1.00	1.00	1.00	A1	1.00	0.66	1.00	B2
CY0110_21335	A3IRH1	Uncharacterized protein	1.00	0.36	0.09	C1	0.27	0.31	1.00	B2
CY0110_30411	A3IRY1	Uncharacterized protein	1.00	1.00	3.76	B1	1.00	1.00	1.00	A2
CY0110_20695	A3IU26	Uncharacterized protein	1.00	1.00	1.00	A1	1.56	1.00	1.00	A2
CY0110_25211	A3IUK3	Uncharacterized protein	1.00	1.00	6.63	B1	1.00	1.00	1.00	A2
CY0110_09081	A3IVD9	Uncharacterized protein	1.00	1.00	1.00	A1	1.00	1.00	0.28	A2
CY0110_20540	A3IW25	Uncharacterized protein	1.00	1.00	0.13	C1	0.28	0.26	1.00	B2
CY0110_09435	A3IXM5	Uncharacterized protein	1.00	1.00	0.25	C1	0.37	0.41	0.47	B2
CY0110_27909	A3IXQ2	CsbD-like protein	1.00	1.00	1.00	A1	0.42	1.00	1.00	A2
CY0110_23348	A3IPG1	Uncharacterized protein	1.00	1.00	2.51	B1				
CY0110_11443	A3IVT9	Rhodanese-like protein	1.00	1.00	7.37	B1				

[a] Proteins with ratio ≠ 1.00 are considered differently expressed according to the stringent criteria defined in this work (see Material and methods) [25]. For easier interpretation of the data, the fold-change values of proteins that did not passed the significance threshold criteria were set to 1.00.
[b] Accession number according to UniProt database.
[c] Protein name according to UniProt database.
[d] Cluster membership according to the hierarchical cluster analysis performed with all ratios (i.e. not only metal-exposed/control, but also metal-exposed 1/ metal-exposed 2). The number of unique peptides and peptides spectral matches is provided in Mota et al. [28].

The relative levels of glutamine synthetase (GS), the key enzyme involved in amino acid/nitrogen metabolism, increased after chronic Cd^{2+} exposure.

Although only four proteins involved in nucleotide sugar metabolism were identified, their levels were unchanged in all metal-exposed conditions. These results are consistent with the constant rate of RPS production observed for metal-supplemented cultures of *Cyanothece*.

The abundance of most of the chaperones identified did not change in Cd^{2+} stress conditions, with the exception one of the GroEL isoforms, which was present in higher levels in 20 days and acute Cd^{2+} exposure and the DnaK which was present in higher levels in acute Cd^{2+} exposure. The abundance of these proteins and GroES was also affected by Cu^{2+}, with increased levels at 10 days and different fold changes in acute exposure.

Regarding the cell's anti-oxidative defenses, the levels of two ferritin and Dps proteins were differentially altered in 20 days Cd^{2+} exposure, while the abundance of rehydrin decreased in all metal-exposed cells. SOD and a thioredoxin increased in Cu^{2+} acute stress conditions.

A couple of proteins involved in the acquisition and metabolism of inorganic nutrients such as sulfur and iron increased in Cu^{2+} acute stress, while four proteins involved in translation were differentially expressed. Moreover, two ribosomal proteins decrease and a long-chain-fatty-acid CoA ligase increased in Cd^{2+} chronic exposed cells.

It is worth to notice that the levels of 22 uncharacterized proteins were also affected by metal stress.

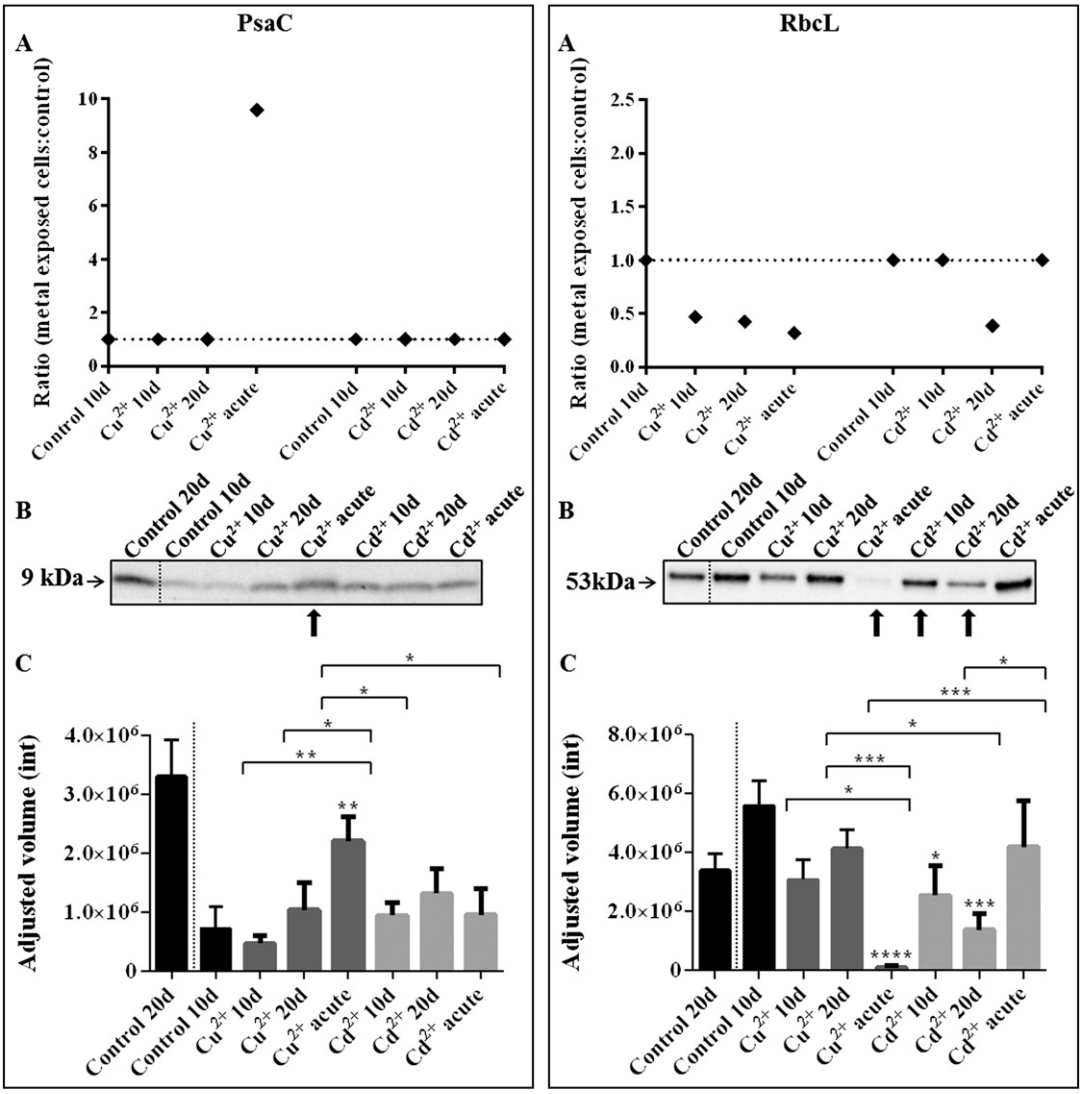

Fig. 8 – Quantitative analysis of the PSI component PsaC and of the large subunit of RuBisCO — RbcL. *Cyanothece* cells were grown in ASNIII buffered medium (control 10 and 20 days), or buffered medium supplemented with 0.1 mg/l of Cu^{2+} or 5 mg/l of Cd^{2+} (for 10 or 20 days, chronic exposure) or 1 mg/l of Cu^{2+} or 50 mg/l of Cd^{2+} (24 h, acute exposure). (A) Results obtained in iTRAQ study 1 — Cu^{2+} exposure and study 2 — Cd^{2+} exposure. (B) Western blot analysis of the relative amounts of PsaC or RbcL (the membranes shown here are representative of three independent experiences), arrows indicates the band with significant higher/lower intensities. (C) Quantification of the intensity of the bands, expressed as adjusted band volume according to the Image Lab™ software (Bio-Rad). To facilitate comparison of data, results from 20 days control cultures – absent in iTRAQ – are separated by a dash line. Data are means ± standard deviations (n = 3). Statistically significant differences are identified: * ($P < 0.05$), ** ($P < 0.01$), * ($P < 0.005$) and **** ($P < 0.001$).**

3.4. *iTRAQ validation studies: PsaC and RbcL relative levels, ROS content, SOD activity and O_2 evolution measurements*

Western blot analyses were performed to further confirm the fold change directions observed for PsaC and RbcL in the iTRAQ studies. In general, the data obtained are in agreement with that of the iTRAQ; the levels of the PSI component PsaC were shown to increase significantly in Cu^{2+} acute stress (Fig. 8), whereas the levels of RuBisCo decreased in acute Cu^{2+} exposure, as well as in 20 days chronic Cd^{2+} stress (Fig. 8). The decrease in RuBisCo observed for Cu^{2+} chronic exposure in iTRAQ study 1 is also observed in the Western blot although not statistically significant.

Given the effects of the metals in the abundance of several proteins involved in cell redox homeostasis, the levels of intracellular ROS and the activity of SOD were also assessed (Fig. 9). The amount of the fluorescent probe, and thus of ROS, was significantly higher in Cd^{2+} 20 days chronic exposure (Fig. 9). Concerning SOD, gel zymography assays revealed that the activity of this enzyme increases in Cu^{2+} acute stress and in 20 days and acute Cd^{2+} exposure. However, these results are only supporting iTRAQ study 1 since no variation was observed for the levels of SOD in iTRAQ study 2.

The levels of O_2 evolution drastically decreases when the cells are exposed to Cu^{2+} for 10 days but it is possible to observe a recovery after 20 days (Fig. 10). The effects of Cu^{2+}

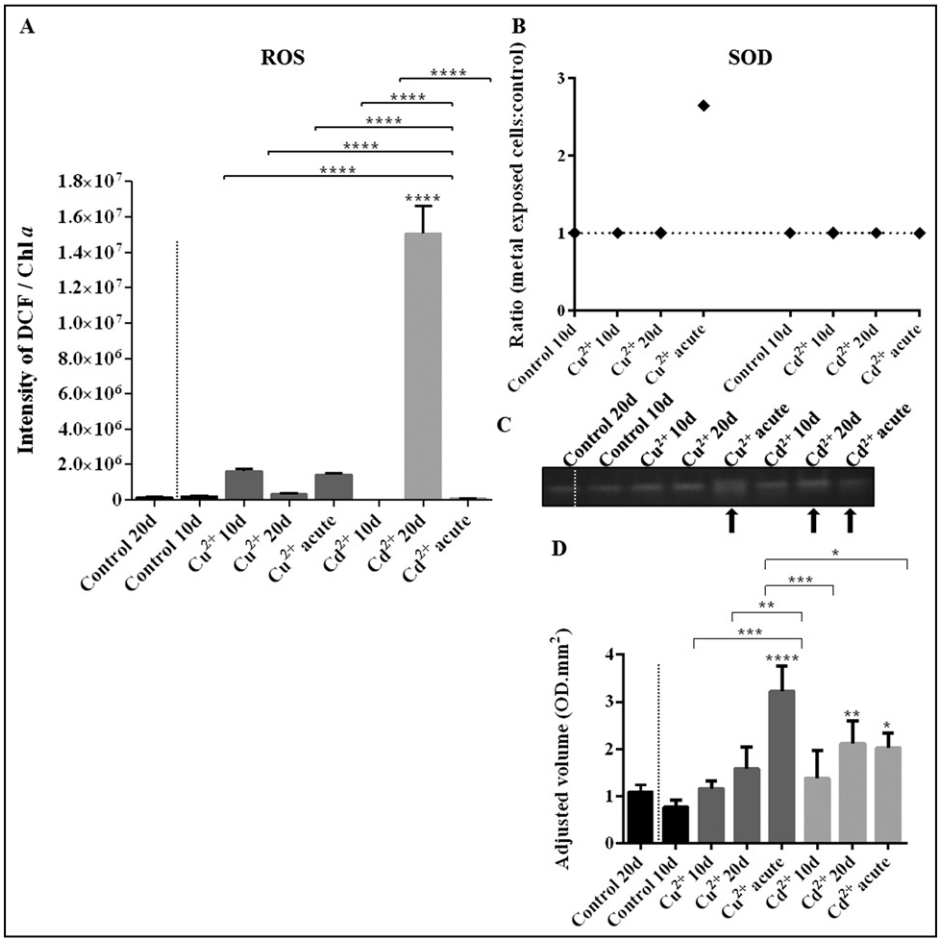

Fig. 9 – In vivo detection of reactive oxygen species (ROS) and superoxide dismutase (SOD) activity measurements. *Cyanothece* cells grown in ASNIII buffered medium (control 10 and 20 days), or buffered medium supplemented with 0.1 mg/l of Cu^{2+} or 5 mg/l of Cd^{2+} (for 10 or 20 days, chronic exposure) or 1 mg/l of Cu^{2+} or 50 mg/l of Cd^{2+} (24 h, acute exposure). (A) Relative levels of ROS expressed as intensity of the fluorescent probe H2DCF-DA (counts per second) per amount of chlorophyll *a*. (B) Results obtained for SOD in iTRAQ study 1 — Cu^{2+} exposure and study 2 — Cd^{2+} exposure. (C) Gel zymography analysis of SOD activity (the gel shown here is representative of three independent experiences), arrows indicate the bands with significant higher intensity. (D) Quantification of the intensity of the bands obtained in SOD gel zymography assays according to the Quantity One® 1-D analysis software (Bio-Rad). To facilitate comparison of data, results from 20 days control cultures – absent in iTRAQ – are separated by a dash line. Data are means ± standard deviations (n = 3). Statistically significant differences are identified: * ($P < 0.05$), ** ($P < 0.01$), * ($P < 0.005$) and **** ($P < 0.001$).**

acute exposure were much more severe with no net O_2 evolution observed, similar to what was observed for Cd^{2+} (Fig. 10).

4. Discussion

The different tolerances exhibited by *Cyanothece* cells grown in the presence of the metals studied ($Cu^{2+} < Pb^{2+} < Cd^{2+} < Li^{+}$) are probably related to the specific nutritional requirements/mechanisms of metal uptake and accumulation in the cells [14,29].

The addition of 0.1 mg of copper per l of culture medium affected negatively the growth of *Cyanothece* cells. Similar concentrations had also toxic effects in *Spirulina platensis*-S5 [30] *Nostoc punctiforme* PCC 73120 cells [31], and *Gloeothece* sp. PCC 6909 [32]. Cu^{2+} is an essential micronutrient that acts as a cofactor for several proteins/enzymes, such as plastocyanin and cytochrome *c* oxidase, involved in the oxygenic photosynthetic electron transfer chain [33,34]. Therefore, in contrast with other bacteria in which most of Cu^{2+}-containing proteins are located in the plasma membrane or the periplasm, in cyanobacteria this metal is required at the thylakoid level, which imposes further complexity to its homeostasis [33–36]. In cyanobacteria, Cu^{2+} is imported into the cell by a P_1-type ATPase (CtaA), then chaperoned by Atx1 until the thylakoids, and finally transported into the thylakoids lumen by a second P_1-type ATPase (PacS) [33,35–37]. However, it is well established that an excess of Cu^{2+} can be toxic to the cells by promoting the generation of ROS and/or competing for the binding sites of

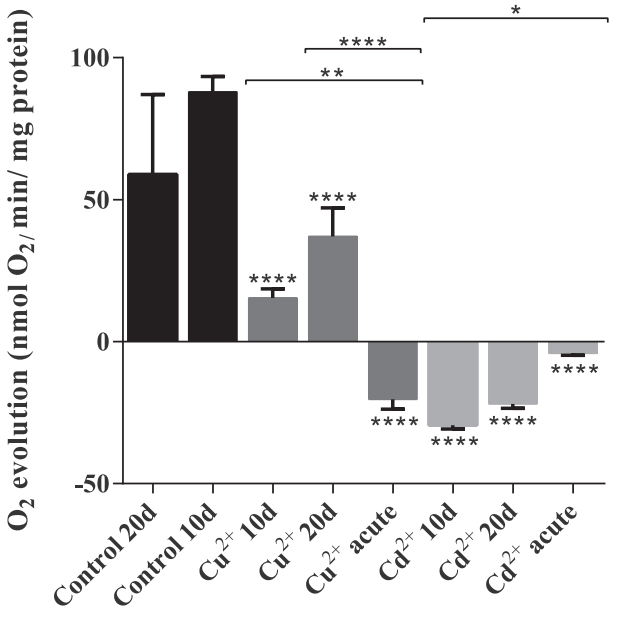

Fig. 10 – O_2 evolution measurements. *Cyanothece* cells were grown in ASNIII buffered medium (control 10 and 20 days), or buffered medium supplemented with 0.1 mg/l of Cu^{2+} or 5 mg/l of Cd^{2+} (for 10 or 20 days, chronic exposure) or 1 mg/l of Cu^{2+} or 50 mg/l of Cd^{2+} (24 h, acute exposure). To facilitate comparison of data, results from 20 days control cultures – absent in iTRAQ – are separated by a dash line. Results are expressed as nmol O_2/ min/ mg protein. Data are means ± standard deviations (n = 3). Statistically significant differences are identified: * ($P < 0.05$), ** ($P < 0.01$), and ** ($P < 0.001$).**

metallothioneins harboring other metals, impairing cell function and eventually causing cell death [29,38]. To cope with the excess of Cu^{2+}, bacterial cells developed several efflux mechanisms to regulate its intracellular concentration [39]. In cyanobacteria, one family of cation-transporting CPx-type ATPases is proven to be involved in the export of Cu^{+} [15]. Moreover, in *Synechocystis* sp. PCC 6803, it was shown that a two-component system (CopRS) is essential for copper resistance by regulating the expression of a Cu^{2+} efflux system (HME-RND: heavy-metal resistance-nodulation-cell division) [35].

The addition of 1 mg/l of lead resulted in growth impairment of *Cyanothece* cells. The effect of this sub-lethal concentration was previously observed in *Anabaena flos-aquae* [40], and in *Spirulina platensis*-S5 concentrations down to 0.2 mg/l also affected growth [30]. In contrast, for *Gloeothece* sp. PCC 6909 and its sheathless mutant CCY 9612 the effects of the presence of the metal were only observed for concentrations of 10 mg/l and 20 mg/l, respectively [32]. The authors also demonstrated that the RPS of these strains have a high affinity to Pb^{2+} what could explain the higher tolerance. Pb^{2+} has no known biological function and its toxicity has been linked to the inactivation of the cellular antioxidant pool and disruption of metabolic balance leading to inhibition of photosynthetic activity [30,32,40–42]. However, the mechanisms by which the metal enters the cells are not fully characterized, but one possible explanation is that the uptake of Pb^{2+} is performed by unspecific binding to importing ATPases [39]. In bacteria, two DNA-binding Cd^{2+}/Pb^{2+}-sensing transcriptional repressors (CadC and CmtR) are described to trigger the de-repression of genes encoding proteins involved in the export of these ions [36,39]. In cyanobacteria, another family of CPx-type ATPases, than the one mentioned above, it is known to be involved in the export of divalent cations such as Pb^{2+} and Cd^{2+} [15].

In our study, levels of cadmium higher than 3 mg/l influenced negatively *Cyanothece* growth, while for *Nostoc punctiforme* PCC 73120 [31], *Anabaena flos-aquae* [40] and *Microcystis aeruginosa* Kütz 854 [43] one order of magnitude lower concentrations were found to be lethal. Cd^{2+} is a non-essential metal with an uptake system barely understood. In bacteria and plants, it is described that Cd^{2+} can enter the cell by uptake systems used by other cations, such as magnesium, manganese and calcium [29]. The cells tolerance to Cd^{2+} can be due to mechanisms already discussed above for other metals, but also be achieved by binding to metallothioneins. In bacteria, the first metallothionein to be characterized was a Cd^{2+} binding protein found in the unicellular cyanobacterium *Synechococcus* sp. [29,44].

Cyanothece growth was barely affected by the presence of lithium, only concentrations as high as 70 mg/l resulted in cell dead. There is not much information about Li^{+} biological function and/or uptake and efflux in cyanobacterial cells. One study in *Synechocystis* sp. PCC 6803 hypothesized that Li^{+}, and other chemically similar monovalent cations, could be uptaken via a potassium transport system [45].

Overall, *Cyanothece* cells are able to cope with different metals/different metal concentrations. Most probably, the high amount of RPS present in the medium contributes to this tolerance, since a positive correlation between EPS production and metal tolerance has been observed for other cyanobacteria [46,47]. It is worthwhile to mention that *Cyanothece* is one of most efficient RPS producers [17]. These polymers, with their overall anionic charge constitute an effective sink decreasing the amount of metal in solution [8,32]. In addition, a recent work has demonstrated that EPS can also protect the cells from metal toxicity by an indirect mechanism that involves Fe homeostasis [48].

The ultrastructural changes observed by TEM in *Cyanothece* cells grown in the presence of metals, namely the increase of the intrathylakoidal space and the formation of thylakoid membrane vesicles (Fig. 3), are similar to the ones observed for several cyanobacterial strains exposed to other stress factors such as high light intensities or changes in the wavelength [49]. Indeed, as observed for high light intensities, the presence of heavy metals is known to induce a change in the redox status of the electron transport chain, which influences the structure and functional organization of the thylakoids [14]. In addition, a higher number of inclusions were also observed. Ultrathin sections of other cyanobacterial strains grown in the presence of Pb^{2+} or Cu^{2+} also showed expanded thylakoids and an increase in inclusions/polyphosphate bodies [32,50]. Polyphosphate, which has a negative surface charge can provide binding sites for heavy metals, helping in the detoxification of metals [9]. No intracellular sites of metal accumulation were detected by EDX spectroscopy in *Cyanothece* cells (Fig. 4), most probably due to the reduced sub-lethal metal concentrations added to the cultures. In agreement, Maldonado et al. only observed intracellular accumulation of Pb^{2+} in different

cyanobacteria by increasing the concentration of the metal up to 10 mM [50]. Another plausible reason is the existence of efficient metal efflux systems, that allow the cells to cope with metal toxicity at the concentrations/time-points tested. The results from atomic absorption spectroscopy corroborate this hypothesis.

The comparison of the proteomes of cells grown in the absence or presence of an essential metal (Cu^{2+}) and a non-essential metal (Cd^{2+}) was performed by iTRAQ. The inclusion of the same control replicates in study 1 (Cu^{2+} exposure) and study 2 (Cd^{2+} exposure) allows the direct comparison of the data between studies (see Fig. 1).

Regarding study 1, the acute exposure was the condition that promoted more quantitative changes and stronger O_2 evolution impairment, despite the modest growth inhibition observed 24 h after adding the Cu^{2+} to the culture. This strongly suggests that the cells are already coping with the metal, as supported by TEM and atomic absorption spectroscopy results. Conversely, the higher number of proteins with unchanged levels after 10 and 20 days chronic Cu^{2+} exposure suggests that those conditions are less severe to the cells, allowing the growth recovery observed at day 20. Similar growth recovery has been observed for *Anabaena doliolum* exposed to Cu^{2+}, and this recovery was correlated with a decrease of the intracellular concentration of the metal [51]. Metal efflux is recognized as the main bacterial resistance mechanism to overcome the toxicity of transition metal ions [52]. After 24 h of acute Cu^{2+} stress, the levels of the majority of PBS components were unchanged, whereas the levels of several PSI and PSII proteins increased. On the other hand, the O_2 evolution rate ceases as previously observed in other cyanobacteria [51,53]. Thus, it is possible that the increased levels of PSI and PSII proteins arise from the need to replace inactivated PS components. The increase of plastocyanin levels is one of the strategies used by the cells to reduce the free intracellular Cu^{2+} concentration, with this Cu^{2+}-containing protein replacing cytochrome C_6 in the electron transfer [36,54–56]. The concomitant increase in the levels of the alpha and beta subunits of ATP synthase and decrease of the FNR abundance strongly points towards an imbalance of the ATP:NADPH ratios. This assumption is consistent with the lower abundance of the RuBisCO large subunit. Likewise, the lower levels of glycolysis-related proteins suggest a decrease in the metabolic flux through this pathway, which results in lower amounts of phosphoenolpyruvate for the tricarboxylic acid (TCA) cycle, and consequently less 2-oxoglutarate (2-OG) [57]. This compound was identified as metabolic signal for controlling the carbon:nitrogen balance of the cells, linking carbohydrate metabolism to nitrogen assimilation [58]. Therefore, it is likely that nitrogen fixation is somehow impaired, even if the levels of the GS did not change according to the stringent criteria of significance imposed in this work [25]. The metabolic rearrangements discussed above may result in an energy investment in metal extrusion and are in agreement with the previous reported low intracellular levels of ATP in Cu^{2+} exposed cells [51]. By comparing the results obtained for Cu^{2+} acute and chronic exposure, it is possible to predict a recovery of photosynthetic activity during chronic exposure, as supported by the unchanged levels of PSI and PSII components and an increase in O_2 evolution from 10 to 20 days. Most probably, the lower abundance of PBS also contributes to this recovery, by allowing the cells to reduce the amount of energy that reaches the photosynthetic apparatus, thus preventing and/or minimizing ROS-induced damages [16,55]. This prediction is also supported by the reduction in the number of proteins involved in carbohydrate metabolism in Cu^{2+} chronic exposure compared to the control, although the levels of RbcL are still lower. The degradation of PBS also releases cellular components, which can be recycled and used in the production of proteins necessary for Cu^{2+} detoxification.

The levels of chaperones during Cu^{2+} exposure are also affected. Chaperones are known to mediate the correct assembly of several polypeptides [59]. In cyanobacteria, the heat-shock proteins GroEL and GroES are the most prominent chaperones, being up-regulated in a need-based manner [60]. The increased levels of GroES in Cu^{2+} acute stress strongly suggest that this protein is involved in the mitigation of the metal toxic effects. Conversely, the lower levels of both GroEL isoforms are in contrast with previous works that report increased GroEL levels under this stress condition [61]. It is possible that under metal stress these proteins might undergo a different time-dependent induction, with GroES being induced prior to GroEL. The fold changes observed for these proteins in cells exposed to 10 days chronic Cu^{2+} stress further support this assumption. Regarding DnaK, the unchanged levels observed after acute Cu^{2+} stress and higher abundance after 10 days chronic exposure may be an indication that this protein is involved in long-term Cu^{2+} resistance. Noteworthy, the increased levels of a yet uncharacterized chaperon in acute Cu^{2+} conditions may unveil a new player in the mitigation of the effects resulting from metal stress.

As expected, Cu^{2+} exposure also lead to an unbalance of ROS. The increased levels and activity of *Cyanothece* FeSOD in Cu^{2+} acute conditions emphasize the stress imposed by the metal to PS machinery, and is in agreement with that described for other cyanobacteria grown in contact with heavy metals [30,51,62–65].

Ten days chronic and acute Cu^{2+} exposure also affected the metabolism of other inorganic elements, such as sulfur, phosphate and iron. The changes in the levels of sulfur- and iron-related proteins may be related with an increased demand for these two elements, in order to synthesize or repair damaged Fe-S clusters, including those present in PS components [55,66]. However, further analysis needs to be carried out to elucidate these interactions.

Concerning Cd^{2+} exposure, the results differ substantially of those obtained for Cu^{2+}. During the chronic exposure the cells seem to accumulate damages and a recovery is not observed as for Cu^{2+}. In contrast, after acute exposure the levels of most proteins remained unchanged. TEM results showed that after 24 h acute metal exposure cells have already ultrastructural changes at the thylakoid level, as supported by the impairment in O_2 evolution, although the modest growth inhibition and the proteome data suggest that these effects are still insufficient to trigger a significant activation of metal detoxification mechanisms and impair growth. The decreased levels of PBS components in Cd^{2+} chronic exposure are consistent with the need to recycle protein components, as previously suggested for similar conditions [43,55,62]. The unchanged levels of PSI and PSII

components in all Cd^{2+}-exposed conditions, together with the impairment in O_2 evolution, are in agreement with reports that indicate that the site for Cd^{2+}-induced inhibition of photosynthesis is beyond PSI [43,67]. Despite that, the key target is controversial, with some studies suggesting that the metal interacts with the sulfhydryl groups of FNR, while others rule it out as primary target [43,67]. Our data is consistent with a time-dependent degradation of FNR, consequently decreasing NADPH availability. The decrease of plastocyanin levels strongly suggests this protein is not the main electron carrier between cytochrome b_6f complex and PSI in Cd^{2+} exposure conditions. Regarding carbohydrate metabolism, the lower levels of RcbL after 20 days chronic Cd^{2+} exposure are consistent with a long term negative effect in CO_2 fixation. This decrease in carbon assimilation seems to be a widespread response of cyanobacteria to Cd^{2+} exposure [52,62,67,68]. On the other hand, the effects of this metal on other carbohydrate metabolic pathways are more difficult to predict. The decreased levels of fructose-biphosphatase aldolase and phosphoglycerate kinase, in all Cd^{2+} conditions, seem to point out to a metal-induced reorganization of the carbon flux. Regarding the first enzyme, it is possible that Cd^{2+} replaces Zn^{2+} in the enzyme active center, as previously observed for *Escherichia coli* [69]. This overall shift in the route followed by carbon compounds seems to be more accentuated after 20 days chronic stress, as suggested by the higher levels of glucose-6-phosphate isomerase. Previous works on Cd^{2+}-induced toxicity in cyanobacteria indicate a decrease in carbohydrate metabolism, which extends to nitrogen assimilation to save energy and reducing power and prevent the poisoning incorporation of Cd^{2+} in metalloenzymes [52,62,68]. On the contrary, in this work, the levels of GS were shown to increase after chronic exposure to Cd^{2+}, remaining unchanged after acute stress. Nonetheless, it is important to point out that those studies were performed in other cyanobacterial strains and that the period of metal-exposure was always considerably shorter, usually up to 48 h. Overall, the data obtained here for *Cyanothece* are consistent with a time-dependent increase in nitrogen assimilation.

As observed for Cu^{2+}-exposure conditions, the levels of one GroEL and DnaK changed after Cd^{2+} exposure, suggesting that these chaperones are also involved in the response to Cd^{2+}. However, the higher abundance of these proteins in acute stress conditions, points out to a rapid activation of their regulatory mechanisms, rather than the time-independent induction observed for Cu^{2+}. Although the levels of the majority of the proteins involved in ROS detoxification was unchanged after chronic exposure to Cd^{2+} (including SOD), the increased ROS levels after 20 days chronic stress and higher SOD activity in both 20 days chronic and 24 h acute exposure, unequivocally show that Cd^{2+} affects ROS homeostasis. The high extent of the cellular damages under these conditions is also evident in the high levels of a long-chain-fatty acid CoA ligase, which is involved in the activation of long-chain fatty acids for synthesis and degradation of cellular lipids, including the activation of endogenous free fatty acids released from membrane lipids [70].

5. Conclusions

Our study demonstrates that different heavy metals affect *Cyanothece* sp. CCY 0110 cells differently, and the response triggered to cope with these metals is also quite distinctive. Independently of the metal tested, sub-lethal concentrations affect the photosynthesis/photosynthetic apparatus with visible ultrastructural changes mainly at the thylakoid level. The comparison of the proteomes allowed to follow the kinetic of stress responses and to distinguish specific effects related to the time of exposure and/or the concentration of the metals. Regarding Cu^{2+}, it seems that the cells tune down their metabolic rate, including O_2 evolution, CO_2 fixation and N_2 assimilation to invest the spare energy in the activation of metal detoxification mechanisms, which ultimately results in a remarkable recovery. In contrast, the toxic effects of Cd^{2+} accumulate over time preventing recovery. It is likely that the lower amount of energy available upon Cd^{2+} exposure (due to an increase in N_2 assimilation without the concomitant boost in photosynthetic-driven ATP synthesis) contributes to the lower efficiency of the mechanisms of Cd^{2+} detoxification compared to those of Cu^{2+}. However, one should also bear in mind that Cd^{2+} is a non-essential metal and therefore the cells might not have the same capacity to deal with it. Despite the different effects of the different metals/metals concentrations and physiological responses of the cells, the amount of RPS produced still follows the growth pattern, suggesting that the relationship between central carbon metabolic pathways and EPS production is not straightforward.

Supplementary data to this article can be found online at http://dx.doi.org/10.1016/j.jprot.2015.03.004.

Transparency document

The Transparency document associated with this article can be found, in the online version.

Acknowledgments

This work was funded by FEDER Funds through the Operational Competitiveness Programme — COMPETE and by national funds through FCT — Fundação para a Ciência e a Tecnologia under the project FCOMP-01-0124-FEDER-028314 (PTDC/BIA-MIC/2889/2012) and the scholarships SFRH/BD/84914/2012 and SFRH/BDP/72400/2010. We thank Professor Lucas Stal for providing *Cyanothece* sp. CCY 0110. Sheffield acknowledges the EPSRC (EP/E036252/1).

REFERENCES

[1] Li P, Harding SE, Liu Z. Cyanobacterial exopolysaccharides: their nature and potential biotechnological applications. Biotechnol Genet Eng Rev 2001;18:375–404.
[2] Pereira S, Zille A, Micheletti E, Moradas-Ferreira P, De Philippis R, Tamagnini P. Complexity of cyanobacterial exopolysaccharides: composition, structures, inducing

factors and putative genes involved in their biosynthesis and assembly. FEMS Microbiol Rev 2009;33:917–41.
[3] Valko M, Morris H, Cronin MT. Metals, toxicity and oxidative stress. Curr Med Chem 2005;12:1161–208.
[4] Jarup L. Hazards of heavy metal contamination. Br Med Bull 2003;68:167–82.
[5] Micheletti E, Pereira S, Mannelli F, Moradas-Ferreira P, Tamagnini P, De Philippis R. Sheathless mutant of cyanobacterium *Gloeothece* sp. strain PCC 6909 with increased capacity to remove copper ions from aqueous solutions. Appl Environ Microbiol 2008;74:2797–804.
[6] Parikh A, Madamwar D. Partial characterization of extracellular polysaccharides from cyanobacteria. Bioresour Technol 2006;97:1822–7.
[7] De Philippis R, Micheletti E. Heavy metal removal with exopolysaccharide-producing cyanobacteria. In: Wang LK, Chen JP, Hung YT, Shammas NK, editors. Heavy Metals In The Environment. Boca Raton, USA: CRC Press; 2009. p. 89–122.
[8] De Philippis R, Colica G, Micheletti E. Exopolysaccharide-producing cyanobacteria in heavy metal removal from water: molecular basis and practical applicability of the biosorption process. Appl Microbiol Biotechnol 2011;92:697–708.
[9] Fiore MF, Trevors JT. Cell composition and metal tolerance in cyanobacteria. Biometals 1994;7:83–103.
[10] Malik A. Metal bioremediation through growing cells. Environ Int 2004;30:261–78.
[11] Lewinson O, Lee AT, Rees DC. A P-type ATPase importer that discriminates between essential and toxic transition metals. Proc Natl Acad Sci U S A 2009;106:4677–82.
[12] Ishaque AB, Johnson L, Gerald T, Boucaud D, Okoh J, Tchounwou PB. Assessment of individual and combined toxicities of four non-essential metals (As, Cd, Hg and Pb) in the microtox assay. Int J Environ Res Public Health 2006;3:118–20.
[13] Valls M, de Lorenzo V. Exploiting the genetic and biochemical capacities of bacteria for the remediation of heavy metal pollution. FEMS Microbiol Rev 2002;26:327–38.
[14] Baptista MS, Vasconcelos MT. Cyanobacteria metal interactions: requirements, toxicity, and ecological implications. Crit Rev Microbiol 2006;32:127–37.
[15] Nies DH. Efflux-mediated heavy metal resistance in prokaryotes. FEMS Microbiol Rev 2003;27:313–39.
[16] Latifi A, Ruiz M, Zhang CC. Oxidative stress in cyanobacteria. FEMS Microbiol Rev 2009;33:258–78.
[17] Mota R, Guimaraes R, Buttel Z, Rossi F, Colica G, Silva CJ, et al. Production and characterization of extracellular carbohydrate polymer from *Cyanothece* sp. CCY 0110. Carbohydr Polym 2013;92:1408–15.
[18] Rippka R, Deruelles J, Waterbury JB, Herdman M, Stanier RY. Generic assignments, strain histories and properties of pure cultures of cyanobacteria. J Gen Microbiol 1979;111:1–61.
[19] Anderson SL, McIntosh L. Light-activated heterotrophic growth of the cyanobacterium *Synechocystis* sp. strain PCC 6803: a blue-light-requiring process. J Bacteriol 1991;173:2761–7.
[20] Meeks JC, Castenholz RW. Growth and photosynthesis in an extreme thermophile, *Synechococcus lividus* (Cyanophyta). Arch Mikrobiol 1971;78:25–41.
[21] Dubois M, Gilles KA, Hamilton JK, Rebers PA, Smith F. Colorimetric method for determination of sugars and related substances. Anal Chem 1956;28:350–6.
[22] Seabra R, Santos A, Pereira S, Moradas-Ferreira P, Tamagnini P. Immunolocalization of the uptake hydrogenase in the marine cyanobacterium *Lyngbya majuscula CCAP 1446/4* and two *Nostoc* strains. FEMS Microbiol Lett 2009;292:57–62.
[23] Pereira SB, Ow SY, Barrios-Llerena ME, Wright PC, Moradas-Ferreira P, Tamagnini P. iTRAQ-based quantitative proteomic analysis of *Gloeothece sp. PCC 6909*: comparison with its sheathless mutant and adaptations to nitrate deficiency and sulfur limitation. J Proteomics 2011;75:270–83.
[24] Chong PK, Gan CS, Pham TK, Wright PC. Isobaric tags for relative and absolute quantitation (iTRAQ) reproducibility: implication of multiple injections. J Proteome Res 2006;5:1232–40.
[25] Pham TK, Roy S, Noirel J, Douglas I, Wright PC, Stafford GP. A quantitative proteomic analysis of biofilm adaptation by the periodontal pathogen *Tannerella forsythia*. Proteomics 2010;10:3130–41.
[26] Leitao E, Oxelfelt F, Oliveira P, Moradas-Ferreira P, Tamagnini P. Analysis of the *hupSL* operon of the nonheterocystous cyanobacterium *Lyngbya majuscula CCAP 1446/4*: regulation of transcription and expression under a light-dark regimen. Appl Environ Microbiol 2005;71:4567–76.
[27] Lowry OH, Rosebrough NJ, Farr AL, Randall RJ. Protein measurement with the Folin phenol reagent. J Biol Chem 1951;193:265–75.
[28] Mota R, Pereira SB, Meazzini M, Fernandes R, Santos A, Evans CA, et al. Differential Proteomes Of The Cyanobacterium *Cyanothece* sp. CCY 0110 Upon Exposure To Heavy Metals Data In Brief; 2015.
[29] Nies DH. Microbial heavy-metal resistance. Appl Microbiol Biotechnol 1999;51:730–50.
[30] Choudhary M, Jetley UK, Abash Khan M, Zutshi S, Fatma T. Effect of heavy metal stress on proline, malondialdehyde, and superoxide dismutase activity in the cyanobacterium *Spirulina platensis-S5*. Ecotoxicol Environ Saf 2007;66:204–9.
[31] Hudek L, Rai S, Michalczyk A, Rai LC, Neilan BA, Ackland ML. Physiological metal uptake by *Nostoc punctiforme*. Biometals 2012;25:893–903.
[32] Pereira S, Micheletti E, Zille A, Santos A, Moradas-Ferreira P, Tamagnini P, et al. Using extracellular polymeric substances (EPS)-producing cyanobacteria for the bioremediation of heavy metals: do cations compete for the EPS functional groups and also accumulate inside the cell? Microbiology 2011;157:451–8.
[33] De la Cerda B, Castielli O, Durán RV, Navarro JA, Hervás M, De la Rosa MA. A proteomic approach to iron and copper homeostasis in cyanobacteria. Brief Funct Genomic Proteomic 2008;6:322–9.
[34] Shcolnick S, Keren N. Metal homeostasis in cyanobacteria and chloroplasts. Balancing benefits and risks to the photosynthetic apparatus. Plant Physiol 2006;141:805–10.
[35] Lopez-Maury L, Giner-Lamia J, Florencio FJ. Redox control of copper homeostasis in cyanobacteria. Plant Signal Behav 2012;7:1712–4.
[36] Cavet JS, Borrelly GP, Robinson NJ. Zn, Cu and Co in cyanobacteria: selective control of metal availability. FEMS Microbiol Rev 2003;27:165–81.
[37] Robinson NJ, Winge DR. Copper metallochaperones. Annu Rev Biochem 2010;79:537–62.
[38] Tottey S, Patterson CJ, Banci L, Bertini I, Felli IC, Pavelkova A, et al. Cyanobacterial metallochaperone inhibits deleterious side reactions of copper. Proc Natl Acad Sci U S A 2012;109:95–100.
[39] Tottey S, Harvie DR, Robinson NJ. Understanding how cells allocate metals using metal sensors and metallochaperones. Acc Chem Res 2005;38:775–83.
[40] Heng LY, Jusoh K, Ling CH, Idris M. Toxicity of single and combinations of lead and cadmium to the cyanobacteria *Anabaena flos-aquae*. Bull Environ Contam Toxicol 2004;72:373–9.
[41] Burnat M, Diestra E, Esteve I, Sole A. In situ determination of the effects of lead and copper on cyanobacterial populations in microcosms. PLoS One 2009;4:e6204.
[42] Pinchasov Y, Berner T, Dubinsky Z. The effect of lead on photosynthesis, as determined by photoacoustics in *Synechococcus leopoliensis* (cyanobacteria). Water Air Soil Pollut 2006;175:117–25.

[43] Zhou W, Juneau P, Qiu B. Growth and photosynthetic responses of the bloom-forming cyanobacterium *Microcystis aeruginosa* to elevated levels of cadmium. Chemosphere 2006; 65:1738–46.
[44] Turner JS, Robinson NJ. Cyanobacterial metallothioneins — biochemistry and molecular-genetics. J Ind Microbiol 1995;14:119–25.
[45] Avery SV, Codd GA, Gadd GM. Caesium accumulation and interactions with other monovalent cations in the cyanobacterium *Synechocystis* PCC 6803. J Gen Microbiol 1991; 137:405–13.
[46] Ozturk S, Aslim B, Suludere Z. Cadmium(II) sequestration characteristics by two isolates of *Synechocystis* sp. in terms of exopolysaccharide (EPS) production and monomer composition. Bioresour Technol 2010;101:9742–8.
[47] Ozturk S, Aslim B, Suludere Z. Evaluation of chromium(VI) removal behaviour by two isolates of *Synechocystis* sp. in terms of exopolysaccharide (EPS) production and monomer composition. Bioresour Technol 2009;100:5588–93.
[48] Jittawuttipoka T, Planchon M, Spalla O, Benzerara K, Guyot F, Cassier-Chauvat C, et al. Multidisciplinary evidences that *Synechocystis* PCC 6803 exopolysaccharides operate in cell sedimentation and protection against salt and metal stresses. PLoS One 2013;8:e55564.
[49] Baulina OI. Ultrastructural plasticity of cyanobacteria under dark and high light intensity conditions. Ultrastructural Plasticity Of Cyanobacteria. Springer-Verlag Berlin Heidelberg; 2012 11–63.
[50] Maldonado J, Sole A, Puyen ZM, Esteve I. Selection of bioindicators to detect lead pollution in Ebro delta microbial mats, using high-resolution microscopic techniques. Aquat Toxicol 2011;104:135–44.
[51] Bhargava P, Mishra Y, Srivastava AK, Narayan OP, Rai LC. Excess copper induces anoxygenic photosynthesis in *Anabaena doliolum*: a homology based proteomic assessment of its survival strategy. Photosynth Res 2008;96:61–74.
[52] Mehta A, Lopez-Maury L, Florencio FJ. Proteomic pattern alterations of the cyanobacterium *Synechocystis* sp. PCC 6803 in response to cadmium, nickel and cobalt. J Proteomics 2014; 102:98–112.
[53] Dudkowiak A, Olejarz B, Lukasiewicz J, Banaszek J, Sikora J, Wiktorowicz K. Heavy metals effect on cyanobacteria *Synechocystis aquatilis* study using absorption, fluorescence, flow cytometry, and photothermal measurements. Int J Thermophys 2011;32:762–73.
[54] Vermaas WFJ. Photosynthesis and respiration in cyanobacteria. eLS Encyclopedia of Life Sciences. John Wiley & Sons, Ltd; 2001.
[55] DeRuyter YS, Fromme P. Molecular structure of photosynthetic apparatus. In: Herrero A, Flores E, editors. The Cyanobacteria: Molecular Biology, Genomics And Evolution. Norfolk, UK: Caister Academic Press; 2008. p. 217–70.
[56] Zhang L, McSpadden B, Pakrasi HB, Whitmarsh J. Copper-mediated regulation of cytochrome c553 and plastocyanin in the cyanobacterium *Synechocystis* 6803. J Biol Chem 1992;267:19054–9.
[57] Knoop H, Grundel M, Zilliges Y, Lehmann R, Hoffmann S, Lockau W, et al. Flux balance analysis of cyanobacterial metabolism: the metabolic network of *Synechocystis* sp. PCC 6803. PLoS Comput Biol 2013;9:e1003081.
[58] Luque I, Forchhammer K. Nitrogen assimilation and C/N balance sensing. In: Herrero A, Flores E, editors. The Cyanobacteria: Molecular Biology, Genomics And Evolution. Norfolk, UK: Caister Academic Press; 2008. p. 335–82.
[59] Webb R, Sherman LA. The cyanobacterial heat-shock response and the molecular chaperones. In: Bryant DA, editor. The Molecular Biology Of Cyanobacteria. Dordrecht, The Netherlands: Kluwer Academic Publishers; 1994. p. 751–67.
[60] Rajaram H, Chaurasia AK, Apte SK. Cyanobacterial heat-shock response: role and regulation of molecular chaperones. Microbiology 2014;160:647–58.
[61] Castielli O, De la Cerda B, Navarro JA, Hervas M, De la Rosa MA. Proteomic analyses of the response of cyanobacteria to different stress conditions. FEBS Lett 2009;583:1753–8.
[62] Houot L, Floutier M, Marteyn B, Michaut M, Picciocchi A, Legrain P, et al. Cadmium triggers an integrated reprogramming of the metabolism of *Synechocystis* PCC 6803, under the control of the Slr1738 regulator. BMC Genomics 2007;8.
[63] Kumar D, Yadav A, Gaur JP. Growth, composition and metal removal potential of a *Phormidium bigranulatum*-dominated mat at elevated levels of cadmium. Aquat Toxicol 2012;116: 24–33.
[64] Singh VP, Srivastava PK, Prasad SM. Differential effect of UV-B radiation on growth, oxidative stress and ascorbate-glutathione cycle in two cyanobacteria under copper toxicity. Plant Physiol Biochem 2012;61:61–70.
[65] Priya B, Premanandh J, Dhanalakshmi RT, Seethalakshmi T, Uma L, Prabaharan D, et al. Comparative analysis of cyanobacterial superoxide dismutases to discriminate canonical forms. BMC Genomics 2007;8:435.
[66] Giner-Lamia J, Lopez-Maury L, Florencio FJ. Global transcriptional profiles of the copper responses in the cyanobacterium *Synechocystis* sp. *PCC 6803*. PLoS One 2014;9: e108912.
[67] Toth T, Zsiros O, Kis M, Garab G, Kovacs L. Cadmium exerts its toxic effects on photosynthesis via a cascade mechanism in the cyanobacterium, *Synechocystis* PCC 6803. Plant Cell Environ 2012;35:2075–86.
[68] Chen L, Zhu Y, Song Z, Wang J, Zhang W. An orphan response regulator Sll0649 involved in cadmium tolerance and metal homeostasis in photosynthetic *Synechocystis* sp. PCC 6803. J Proteomics 2014;103:87–102.
[69] Hall DR, Kemp LE, Leonard GA, Marshall K, Berry A, Hunter WN. The organization of divalent cations in the active site of cadmium *Escherichia coli* fructose-1,6-bisphosphate aldolase. Acta Crystallogr D Biol Crystallogr 2003;59:611–4.
[70] Kaczmarzyk D, Fulda M. Fatty acid activation in cyanobacteria mediated by acyl-acyl carrier protein synthetase enables fatty acid recycling. Plant Physiol 2010; 152:1598–610.